Draft version February 5, 2008
Preprint typeset using LaTeX style emulateapj v. 6/22/04

REDUCING THE PROBABILITY OF CAPTURE INTO RESONANCE

Alice C. Quillen
Department of Physics and Astronomy, University of Rochester, Rochester, NY 14627 and
Visitor, Research School of Astronomy and Astrophysics, Australian National University, Mount Stromlo Observatory, Cotter Road, Weston Creek, ACT 2611, Australia

Draft version February 5, 2008

ABSTRACT

A migrating planet can capture planetesimals into mean motion resonances. However, resonant trapping can be prevented when the drift or migration rate is sufficiently high. Using a simple Hamiltonian system for first and second order resonances, we explore how the capture probability depends on the order of the resonance, drift rate and initial particle eccentricity. We present scaling factors as a function of the planet mass and resonance strength to estimate the planetary migration rate above which the capture probability drops to less than 1/2. Applying our framework to multiple extra solar planetary systems that have two planets locked in resonance, we estimate lower limits for the outer planet's migration rate allowing resonance capture of the inner planet.

Mean motion resonances are comprised of multiple resonant subterms. We find that the corotation subterm can reduce the probability of capture when the planet eccentricity is above a critical value. We present factors that can be used to estimate this critical planet eccentricity. Applying our framework to the migration of Neptune, we find that Neptune's eccentricity is near the critical value that would make its 2:1 resonance fail to capture twotinos. The capture probability is affected by the separation between resonant subterms and so is also a function of the precession rates of the longitudes of periapse of both planet and particle near resonance.

Subject headings: celestial mechanics

1. INTRODUCTION

Resonances can capture particles in slowly varying dynamical systems. For example, a planet migrating outward can trap planetesimals in resonances exterior to it; as Neptune trapped the Plutinos in the Kuiper belt (e.g., Fernandez & Ip 1984; Malhotra 1995; Hahn & Malhotra 1999; Ida et al. 2000; Chiang & Jordan 2002; Zhou et al. 2002; Levison & Morbidelli 2003; Wyatt 2003). A planet migrating inward can trap planetesimals or planets in resonances interior to it (e.g., Quillen & Holman 2000; Kley et al. 2004). Dust spiraling inward under dissipational forces can become trapped in exterior mean motion resonances with a planet (e.g., Sicardy et al. 1993; Dermott et al. 1994; Marzari & Vanzini 1994; Liou & Zook 1997, 1999; Ozernoy et al. 2000; Wilner et al. 2002; Moro-Martin et al. 2005; Deller & Maddison 2005).

An elegant and predictive theory of resonant capture has been developed for adiabatically varying non-chaotic integrable resonant systems (Yoder 1979; Henrard 1982; Henrard & Lemaitre 1983; Malhotra 1990), and for the same systems but varying with weak nonconservative forces (Gomes 1997). This theory was first applied to systems of tidally locked satellites (Borderies & Goldreich 1984; Peale 1986; Dermott et al. 1988; Malhotra 1990). However this theory does not apply to systems that are near or in the non-adiabatic regime, or are chaotic. Numerical explorations of drifting and migrating systems have revealed differences between measured capture probabilities and those predicted by the adiabatic theory. For dust drifting under dissipational forces, small particles can be drifting sufficiently fast that they are in the non-adiabatic regime. In this case, the capture probability is reduced (e.g., Gomes 1995; Liou & Zook 1999). Numerical simulations of Neptune's migration show that if Neptune migrates rapidly, the capture probability of resonances is reduced (Ida et al. 2000; Friedland 2001; Chiang & Jordan 2002).

In dynamical systems chaotic motion can arise from the overlap of resonances (e.g., Wisdom 1980). Mean motion resonances associated with perturbations by a planet are made up of more than one resonant perturbative term. Holman & Murray (1996) showed how to predict the Lyapunov times of asteroids from the overlap of these resonant terms. The complex behavior of chaotic resonances could influence the way they capture particles when they are varying (e.g., Dermott et al. 1988; Tittemore & Wisdom 1990; Sicardy et al. 1993; Marzari & Vanzini 1994; Quillen 2001). For example, Tittemore & Wisdom (1990) found that the drifting chaotic resonances of the Uranian satellites exhibited different behavior than non-chaotic resonances.

In this paper we strive to develop a general framework that will allow us to better predict the capture probability of resonances. We would like to know when they are likely to capture and how the capture probability depends on the drift or migration rate, resonance order and strength, initial particle orbital elements, and size and separation of subresonances. Some of these parameters depend on the planetary properties and others depend on the particle properties. We would like a flexible framework that could be used to place constraints on migrating planetary extrasolar systems and the properties of the planets and planetesimals residing within them. Previous works have shown how to predict the capture probability as a function of initial particle eccentricity in the adiabatic limit (e.g.,

Electronic address: aquillen@pas.rochester.edu

Henrard 1982; Borderies & Goldreich 1984; Malhotra 1990; Murray & Dermott 1999). Here we strive to understand two regimes that have not been well explored for mean motion resonances. We probe the nonadiabatic regime in which the drift rate is so fast that the resonance can fail to capture. We also explore resonances comprised of multiple resonant subterms.

Our approach is to understand the simplest Hamiltonian model that can illustrate the dynamics of resonance capture. In section 2 we formulate the problem in terms of an idealized Hamiltonian with multiple resonant terms. By rescaling, this simple model allows different resonant systems to be treated in a similar way. In section 3 we consider the system with one resonant term and measure the capture probability as a function of drift rate and initial particle momentum. We extend previous analytical work by Friedland (2001) for the first order resonances and find general expressions that account for trends exhibited by previous simulations (e.g., Wyatt 2003). In section 4 we measure capture probabilities for first and second order resonances containing multiple resonant terms. In section 5 we illustrate how our framework can be applied to planetary systems. A summary and conclusion follows. The appendix lists coefficients for common resonances so that drift rates can be predicted and compared to numerical studies.

2. HAMILTONIAN FORMULATION

We employ the Poincaré coordinates

$$\lambda = M + \varpi, \qquad \gamma = -\varpi$$

and their associated momenta

$$L = \sqrt{GM_* a}, \qquad \Gamma = \sqrt{GM_* a}(1 - \sqrt{1-e^2})$$

where M_* is the mass of the star, λ is the mean longitude, M is the mean anomaly, ϖ is the longitude of pericenter, a is the semimajor axis, and e is the eccentricity. These variables are those describing the orbit of a particle or planetesimal in a plane. The Hamiltonian for the Keplerian system in these coordinates restricted to a plane is

$$H(L,\lambda;\Gamma,\gamma) = -\frac{GM_*}{2L^2} - R$$

where R is the disturbing function that depends on the coordinates of the particle and on the coordinates of the planet. The planet's semimajor axis and mass are denoted a_p and m_p, respectively. The planet's other coordinates are subscripted in the same way. The mean motion of the particle $n = \dot{\lambda}$ where $\dot{\lambda}$ is the derivative with respect to time of λ.

Hereafter we adopt a unit convention with distances in units of the planet's semi-major axis, a_p, at a time t_0. Time is put in units of $\sqrt{a_p^3/GM_*}$. We define μ to be the mass ratio $\mu \equiv m_p/M_*$. At low eccentricity, $\Gamma/L \approx e^2/2$, relating the momentum Γ to the particle eccentricity. We often give the particle semimajor axis in terms of the variable $\alpha \equiv \frac{a_p}{a}$ if $a > a_p$ (external to the planet) and $\alpha \equiv \frac{a}{a_p}$ for $a < a_p$ (internal to the planet).

The unperturbed Hamiltonian or that lacking the disturbing function

$$H_0(L,\lambda;\Gamma,\gamma) = -\frac{1}{2L^2}$$

We consider the the $j : j-k$ exterior mean motion resonance (planet is an interior perturber). We perform a canonical transformation using the mixed variable generating function

$$F_2 = I(j\lambda - (j-k)\lambda_p)$$

leading to new variables

$$I = jL, \qquad \psi = j\lambda - (j-k)\lambda_p$$

and new Hamiltonian

$$H_0'(I,\psi;\Gamma,\gamma) = \frac{-1}{2j^2 I^2} - (j-k)In_p.$$

We now expand around the resonance. Let

$$\Lambda \equiv I - I_0 \tag{1}$$

and

$$\frac{1}{j^2 I_0^3} = (j-k)n_p(t_0).$$

Since we have adopted units $n_p(t_0) = 1$, we find $I_0 = \alpha^{-1/2}/j$ where $\alpha = \frac{a_p}{a} = \left(\frac{j-k}{j}\right)^{2/3}$ on resonance, as expected. Our Hamiltonian now reads

$$K_0(\Lambda,\psi;\Gamma,\gamma) = \text{constant } -(j-k)(n_p-1)\Lambda - \frac{3\Lambda^2}{2j^2 I_0^4}.$$

We can write the unperturbed Hamiltonian as

$$K_0(\Lambda,\psi;\Gamma,\gamma) = a\Lambda^2 + b\Lambda + \text{constant}$$

with coefficients

$$\begin{aligned} a &= -\frac{3}{2}j^2\alpha^2 \\ b &= -(j-k)(n_p-1). \end{aligned} \tag{2}$$

We now recover the disturbing function that is is traditionally expanded as a cosine series of angles in orders of planet and particle eccentricity. We keep the terms inducing precession of the longitude of periapse and low order terms (in eccentricity) containing ψ. The full Hamiltonian

$$\begin{aligned} K(\Lambda,\psi;\Gamma,\gamma) = {} & a\Lambda^2 + b\Lambda + c\Gamma \\ & + \sum_{p=0}^{k} \delta_{k,p}\Gamma^{(k-p)/2}\cos\left(\psi - (k-p)\varpi - p\varpi_p\right) \end{aligned} \tag{3}$$

with coefficient

$$c = -\mu 2 f_2 \alpha^{1/2}. \tag{4}$$

We have used the approximation $e^2 \sim 2\Gamma/L \sim 2\Gamma\alpha^{1/2}$. Here the perturbation strengths, $\delta_{k,p}$, are functions of α, j and Laplace coefficients (see Murray & Dermott 1999). The c term describes secular precession of the longitude of periapse and depends on the function f_2 given in the appendix by Murray & Dermott (1999) and is evaluated at α with index $j = 0$. As have previous studies, we have neglected the dependence of α on time as the planet migrates, and cosine terms from the disturbing function expansion which are expected to average to zero near resonance (e.g., Borderies & Goldreich 1984; Peale 1986; Holman & Murray 1996; Murray & Dermott 1999). The perturbation strengths depend on the planet mass and eccentricity as $\delta_{k,p} \propto \mu e_p^p$. More detailed expressions are listed in the appendix.

The above canonical transformations are similar to those of Holman & Murray (1996) except we have focused on resonances exterior to a planet rather than those interior to it. We have also explicitly kept the $b\Lambda$ term. A system with a migrating planet would be described by a time dependent b coefficient. This allows us to explore the dynamical behavior as particles pass through resonances.

Holman & Murray (1996) showed that the above Hamiltonian is similar to a periodically forced pendulum and that the overlap of the different resonant terms of Equation (3) can induce largescale chaotic behavior. However most previous explorations of resonant capture have only considered one dominant resonant term. When the migration rate is slow, the adiabatic theory developed by (Yoder 1979; Henrard 1982; Borderies & Goldreich 1984; Malhotra 1990; Murray & Dermott 1999) applies. In the next section we explore this simpler situation, but allow the migration rate to be fast or non-adiabatic.

3. PROBABILITY OF CAPTURE IN A SINGLE RESONANCE

In this section we explore the simpler Hamiltonian containing only one dominant resonant term. This situation would be appropriate if the planet's eccentricity is very small in which case the $\delta_{k,0}$ term dominates. The Hamiltonian (Equation 3) including only this term

$$K(\Lambda,\psi;\Gamma,\gamma) = a\Lambda^2 + b\Lambda + c\Gamma + \delta_{k,0}\Gamma^{k/2}\cos\left(\psi - k\varpi\right) \quad (5)$$

It is convenient to perform a canonical transformation with generating function

$$F_2 = J_1\left(\frac{\psi}{k} - \varpi\right) + J_2\psi$$

leading to new variables

$$\frac{J_1}{k} + J_2 = \Lambda, \qquad \phi = \frac{\psi}{k} - \varpi$$
$$J_1 = \Gamma, \qquad \theta = \psi$$

and new Hamiltonian

$$K'(\Gamma,\phi;J_2,\psi) = a\left(\frac{\Gamma^2}{k^2} + J_2^2\right) + \left(\frac{2aJ_2}{k} + \frac{b}{k} + c\right)\Gamma + bJ_2 + \delta_{k,0}\Gamma^{k/2}\cos(k\phi) \quad (6)$$

Note that J_2 is conserved and is small for initial conditions near resonance with small initial eccentricity (or Γ).

Dropping constant terms and setting $b' = (2aJ_2 + b) + kc$, the Hamiltonian in Equation (6)

$$K'(\Gamma,\phi) = \frac{a}{k^2}\Gamma^2 + \frac{b'}{k}\Gamma + \delta_{k,0}\Gamma^{k/2}\cos\left(k\phi\right).$$

By rescaling momentum and time

$$\bar{\Gamma} = \left|\frac{\delta_{k,0}k^2}{a}\right|^{-2/(4-k)}\Gamma$$
$$\tau = |\delta_{k,0}|^{2/(4-k)}\left|\frac{a}{k^2}\right|^{(2-k)/(4-k)}t, \quad (7)$$

we can write this as

$$\bar{K}(\bar{\Gamma},\phi) = \bar{\Gamma}^2 + \bar{b}\bar{\Gamma} + (-1)^k\bar{\Gamma}^{k/2}\cos(k\phi) \quad (8)$$

where

$$\bar{b} = b'|\delta_{k,0}|^{-2/(4-k)}\left|\frac{a}{k^2}\right|^{(k-2)/(4-k)}\mathrm{sign}(a). \quad (9)$$

We relate the drift rate $\dot{b}$ from the migrating planet to that of our scale-free system

$$\left|\frac{d\bar{b}}{d\tau}\right| = \left|\frac{\dot{b}}{k}\right||\delta_{k,0}|^{-4/(4-k)}\left|\frac{a}{k^2}\right|^{2(k-2)/(4-k)}. \quad (10)$$

The form of the Hamiltonian in Equation (8) is (excepting for factors of $\sqrt{2}$)[1] identical to that used to explore capture in the adiabatic limit (e.g., Henrard 1982; Borderies & Goldreich 1984; Malhotra 1990; Murray & Dermott 1999).

3.1. *Capture probability as a function of drift rate and initial momentum for first and second order resonances*

We ask the following question: *Above what drift rate ($\frac{d\bar{b}}{d\tau}$) does the resonance fail to capture?* The system behaves adiabatically when it takes longer than an oscillation period for the system to pass through the resonance. For low initial momentum, the width of the resonance is ~ 1, and the period of oscillation is ~ 1. Consequently we expect the system would evolve adiabatically when $\left|\frac{d\bar{b}}{d\tau}\right| \ll 1$. To go beyond this limit and estimate the probability of capture as a function of drift rate in the non-adiabatic regime, we would need to find solutions to Hamilton's equation. It is non-trivial to find solutions to the equations of motion for Equation (8) when $\bar{b}$ is a function of time and the system is not varying adiabatically (e.g., Friedland 2001). Consequently we have integrated Hamilton's equations of motion numerically to explore the non-adiabatic regime. Once we numerically understand the behavior of the scale-free Hamiltonian (Equation 8), we can make predictions for systems in the same form using the factors of Equation (7).

Our procedure for numerical integration is as follows. Hamilton's equations for Equation (8) are integrated using a conventional Burlisch-Stoer numerical scheme. The initial angle is chosen randomly. We assume that $\bar{b}$ is proportional to time so that only one parameter $\frac{d\bar{b}}{d\tau}$ specifies the time dependence of the system. To ensure that the particles were initially outside of resonance we require the initial value of $|\bar{b}|$ to exceed 1. The parameter $\bar{b}$ was initially chosen to be ~ -15, well outside the resonance. The system passes through resonance when $\bar{b} \sim 0$ so the timescale until capture is $t_{capture} \sim b_{init}(\frac{db}{d\tau})^{-1}$. The system is integrated at least twice the capture time. Two sample integrations are shown in Figure 1. Figure 1a shows an integration illustrating a particle that is captured into resonance and Figure 1b shows one where no capture takes place.

In the adiabatic limit, the capture probability is 1 when the initial particle eccentricity is smaller than a limiting

[1] By rescaling our momentum by a factor of $2^{k+2/(4-k)}$, the Hamiltonian becomes $\bar{\Gamma}^2 + \bar{b}\Gamma + (-1)^k 2^{(k+2)/2}\bar{\Gamma}^{k/2}\cos(k\phi)$ as by Murray & Dermott (1999).

value, e_{lim}, that depends on the order and width of the resonance (e.g., Henrard 1982; Borderies & Goldreich 1984; Malhotra 1990; Murray & Dermott 1999). However when the drift is not adiabatic, the capture probability could depend on the initial particle eccentricity (or momentum $\bar{\Gamma}$) even when it is below this limiting value. Consequently we measured capture probability as a function of both drift rate ($\frac{d\bar{b}}{d\tau}$) and initial particle momentum. For each value of drift rate and initial momentum, we integrated the system 100 times (each time with a different randomly chosen angle) to measure a capture probability.

After the system captures, the momentum increases with time (see Figure 1a) and the resonant angle ϕ librates about a fixed value (0 or π) rather than circulating. If no capture takes place, the momentum jumps as the system pass through resonance (see Fig. 1b). When the momentum increases to a value exceeding the resonance width (approximately 1 as we have rescaled the Hamiltonian) we identify the system as having captured into resonance. We used a limiting value of $\Gamma = 5$ to identify captures. In resonance the angle librates around a fixed value. The condition $\dot{\phi} \sim 0$ implies that $\frac{\partial K}{\partial \Gamma} \sim 0$, and $\bar{\Gamma} \sim -\bar{b}/2$ in resonance. We use this condition to ensure that we integrate Hamilton's equations long enough that the momentum crosses our limiting momentum value when the resonance captures.

Figure 2 and 3 show capture probabilities that we have measured numerically for first and second order resonances ($k = 1$ and 2). In the adiabatic limit for $\bar{\Gamma}(t_0)$ below 3/2 for $k = 1$, or 1/8 for $k = 2$, the capture probability is one.[2] Above these limiting initial momentum values the capture probability is less than 1 in the adiabatic limit. For $\bar{\Gamma}(t_0) = 2.3$, shown as stars in Figure 2, above the limiting value of $\bar{\Gamma}_{0,lim} = 1.5$, we see that the capture probability never reaches 1. At lower drift rates the capture probability approaches a constant value for this initial condition, consistent with the prediction in the adiabatic limit. The same behavior is seen for $k = 2$ with initial momentum $\bar{\Gamma}(t_0) = 1$ (shown as stars in Figure 3). This momentum is eight times the limiting value which ensures capture in the adiabatic limit.

To quantify the width of the probability function, we have fit a function to the capture probability $p(u) = 0.5\left(1 - \tanh\left(\frac{u-u_{1/2}}{w}\right)\right)$ as a function of $u = \log_{10}\left|\frac{db}{d\tau}\right|$. Here $u_{1/2}$ is the log of the drift rate at which the capture probability is 1/2, and w describes the width of the drop. For large w, the slope is shallow, for small w the drop is a steep function of the drift rate. The drift rates at which the capture probability is half and a quarter, and the widths of the probability functions are shown as a function of initial momentum in Figures 4 and 5 for first and second order resonances, respectively. For initial momentum sufficiently low, (e.g., 10^{-2} for $k = 1$ and 10^{-6} for $k = 2$) the drift rate at which the probability is half approaches a limiting value. The steepness of the transition between 100% capture and 0% capture is narrower in its range of drift rates at lower values of initial momentum. The lower the initial momentum, the sharper the transition between a capture probability of 1 and zero. A sharp transition is reached at a lower initial momentum for $k = 2$ than in the $k = 1$ case. For initial momentum near $\bar{\Gamma}_{0,lim}$, the limiting value ensuring capture in the adiabatic limit, there is a regime or a range of drift rates where the capture probability is intermediate. In other words, for $\bar{\Gamma}(t_0) \sim 1$ the widths $w \sim 1$.

We now consider the situation where the transition between a probability of 1 and 0 is sharp. This is true for initial momentum $\bar{\Gamma}(t_0) \lesssim 10^{-2}$ and 10^{-6} for $k = 1$ and for $k = 2$ respectively. For these initial momenta we measure the critical drift rate where the transition takes place. From our numerical integrations, the dynamical system fails to capture for drift rates faster than

$$\left|\frac{d\bar{b}}{d\tau}\right|_{crit} \sim 2.0 \qquad \text{for } k = 1$$
$$\sim 0.25 \qquad \text{for } k = 2. \tag{11}$$

For first order resonances the drift rate for a capture probability of 1/2 is not strongly dependent on the initial momentum as long as this lies below $\bar{\Gamma}_{0,lim}$. However for second order resonances when the initial momentum $\bar{\Gamma}(t_0) \sim 1$, the capture probability of half occurs at a drift rate that is about 10 times that at low initial momentum. We have approximated the dependence of the half probability drift rate on the initial momentum with the following function (shown as a dotted line in Figure 5)

$$\left|\frac{d\bar{b}}{d\tau}\right|_{1/2} \sim 0.25\left(1 + \frac{\bar{\Gamma}(t_0)}{3 \times 10^{-5}}\right)^{0.25}. \tag{12}$$

The power, 0.25, is not necessarily theoretically meaningful. This function is a reasonable match to the measured points of Figure 5 for initial momentum $\bar{\Gamma}(t_0) \lesssim 1$. For higher initial momentum, $\bar{\Gamma}(t_0) \gtrsim 4$, the probability of capture never exceeds 1/2. This initial momentum (4) exceeds $\bar{\Gamma}_{0,lim}$ by a factor of 32.

In the adiabatic limit, the probability of capture drops as a function of increasing momentum (or eccentricity) when the initial momentum is above $\bar{\Gamma}_{0,lim}$. However the probability drops faster for first order resonances than for second order resonances (Hahn & Malhotra 1999). In the adiabatic limit, the probability of capture for a first order resonance drops to 1/2 for $\bar{\Gamma}(t_0) \sim 2.3$ (less than twice the limiting value of 1.5), whereas for second order resonances the probability of capture drops to 1/2 for $\bar{\Gamma}(t_0) \sim 4$ or 32 times the limiting value.

Using the critical drift rates for $\frac{d\bar{b}}{d\tau}$ (equation 11) we can invert Equation (10) to determine which resonances can capture at a particular drift rate. We find that resonances are likely to capture for $\dot{b}$ slower than the critical rates

$$|\dot{b}_{crit}| \sim 2|\delta_{1,0}|^{4/3}|a|^{2/3} \qquad \text{for } k = 1$$
$$\sim \quad 0.5\delta_{2,0}^2 \qquad \text{for } k = 2. \tag{13}$$

Using Equation (2) to replace $\dot{b}$ with the planet's mean motion

$$|\dot{n}_{p,crit}| \sim 2(j-1)|\delta_{1,0}|^{4/3}|a|^{2/3} \qquad \text{for } k = 1$$
$$\sim \quad 0.5(j-2)\delta_{2,0}^2 \qquad \text{for } k = 2. \tag{14}$$

[2] Our momentum is half or 1/4 times that of Murray & Dermott (1999) for $k = 1$ and $k = 2$ respectively. Murray & Dermott (1999) list critical momentum values of 3 and 1/2. These critical values are used to find the maximum particle eccentricity, e_{lim}, that ensures capture in the adiabatic limit (Henrard 1982; Borderies & Goldreich 1984; Malhotra 1990).

For second order resonances, the rate given above can be modified by the function given in Equation (12) to estimate the rate at which the probability is 1/2 as a function of initial momentum;

$$|\dot{n}_{p,1/2}| \sim 0.5(j-2)\delta_{2,0}^2 \left(1 + \frac{\alpha^{-1/2} e_0^2 a}{2.4 \times 10^{-4} \delta_{2,0}}\right)^{0.25} \quad (15)$$

where e_0 is the initial particle eccentricity. This is expression is valid for initial particle eccentricities smaller than $e_0 \lesssim 10 e_{lim}$ where e_{lim} is the eccentricity limit ensuring capture in the adiabatic limit. An expression for e_{lim} is given in the appendix. The factor of 10 comes from the range covered by the function shown in Equation (12). The curve shown in Figure 5 is a reasonable match up to $\Gamma(t_0) \sim 1$ which is approximately $10\bar{\Gamma}_{0,lim}$.

The above relations (Equations 14 and 15) allow us to estimate the likelihood of resonance capture in different astronomical settings. The strength of the perturbative cosine terms ($\delta_{k,p}$) are proportional to the planet's mass or μ, however the critical drift speed depends on $\mu^{4/3}$ for $k = 1$ and on μ^2 for $k = 2$. We see that the critical drift rates for capture are strong functions of the planet mass and this is particularly true for the second order resonances. Slower drift rates are required to allow resonant capture for lower mass planets.

The dependence of critical drift rate on planet mass provides a qualitative explanation for some features of numerical simulations which start with particles in initially low eccentricity orbits. The above relation predicts that only more slowly drifting particles will be able to capture into higher order resonances. We can understand why the 5:3 resonance requires slower migration rates than the 2:1 and 3:2 resonances to capture in the simulations of Wyatt (2003). Although we have integrated a time dependent Hamiltonian system, we can expect similarities between this system and the slowly drifting non-conservative systems. Simulations of dust drifting inward via dissipative forces tend to show that large dust particles are captured into higher order resonances than smaller particles (e.g., Marzari & Vanzini 1994; Liou & Zook 1999). This follows since small particles drift faster than larger ones and the higher order resonances require slower drift rates to capture.

Based on results of simulations of Neptune's migration Ida et al. (2000) proposed that the critical drift rate depended on planet mass to the 4/3 power. They restricted their study to $k = 1$ resonances so their prediction is consistent with our previous equation. This power dependence was confirmed with analytical work by Friedland (2001), also for the $k = 1$ resonance, and numerical work by Wyatt (2003). We confirm the steeper dependence on planet mass of the 5:3 resonance capture probability measured numerically by Wyatt (2003) and specifically predict that the critical drift rate is $\propto \mu^2$ for second order resonances. The relation for the critical drift rate (Equation 14) is both consistent with and more general than the scaling found by these previous studies. Because we have related the critical drift rate (via scaling) to the resonance strengths, the formulation given here can be applied to any first or second order mean motion resonance.

Here we have also found that the probability of capture when the drift is not adiabatic is a non-trivial function of initial particle eccentricity. The transition between a probability of 1 and 0 becomes smoother (covering a larger range of drift rates) as the initial momentum approaches the minimum value ensuring capture in the adiabatic limit (see Figures 2, 3, 4, and 5). For first order resonances, the midpoint drift rate (corresponding to a probability of capture of 1/2) does not significantly depend on the initial particle eccentricity. However for second order resonances the midpoint is at a higher drift rate when the initial momentum or particle eccentricity is higher. The increase in drift rate with initial particle eccentricity allowing capture for second order resonances was described previously by Hahn & Malhotra (2005). However we do not predict the same dependence on resonance width and planet mass. This is because we have restricted our study to initial particle eccentricity near or below e_{lim}, and Hahn & Malhotra (2005) considered initial particle eccentricity exceeding e_{lim}.

Our estimate for the critical drift rate above (Equation 14) is appropriate for a wide range of initial particle eccentricities for first order resonances (as long as they are below the limiting value, e_{lim}). The half probability drift rate's dependence on the initial particle eccentricity can be estimated for second order resonances using Equation (15) when the initial particle eccentricity is lower than ~ 10 times e_{lim}. The framework we provide here can we used to estimate the half probability drift rate for any second order resonance.

Numerical studies report intermediate probabilities for capture into first order resonances from simulations (Ida et al. 2000; Quillen & Holman 2000; Chiang & Jordan 2002; Wyatt 2003). By intermediate, we mean not close to zero or 1, or at a $\sim 50\%$ level. Here we have found that the dynamical system described by Equation (8) for $k = 1$ with only a single resonance term has a limited range of drift rates where the capture probability is intermediate, unless the initial particle momentum $\bar{\Gamma}$ is of order 1. This regime corresponds to an initial particle eccentricity within a factor of a few of e_{lim}, the limiting value ensuring capture in the adiabatic limit. The limiting eccentricity depends on the resonance strength, and planet mass to the power $k/(4-k)$ (using the square root of the scale-free momentum in Equation (7); (Malhotra 1990; Murray & Dermott 1999). For weaker resonances, the initial particle eccentricity limit is more restrictive. It is possible that some of the numerical simulations are effectively in the regime of intermediate capture for certain resonances due to their initial particle eccentricity distribution. We return to this issue in later sections as we identify other regimes of intermediate capture probability for first order resonances.

Though the limiting eccentricity is smaller for second order resonances, the probability of capture drops more slowly in the adiabatic limit as a function of initial particle eccentricity at values above e_{lim}. Furthermore since the half probability drift rate increases with initial particle eccentricity (Equation 15), higher eccentricity particles can be captured at higher drift rates than lower eccentricity particles (as pointed out by Hahn & Malhotra 2005). This also implies that the second order resonances have a larger regime in both range of initial eccentricity and drift rate where the probability of capture is intermediate.

4. THE ROLE OF AN ADDITIONAL RESONANCE TERM

We now consider the differences in the dynamics of capture caused by the addition of a secondary resonant term for a first order resonance. We rescale the momenta and time for Hamiltonian given in Equation (A1) for $k = 1$ according to the Equations(7). This gives us unitless momenta and time

$$\bar{K}_1(\bar{\Lambda}, \psi; \bar{\Gamma}, \gamma) = \bar{\Lambda}^2 + \bar{b}\bar{\Lambda} + \bar{c}\bar{\Gamma} \qquad (16)$$
$$-\bar{\Gamma}^{1/2}\cos(\psi - \varpi) + \bar{\epsilon}\cos(\psi - \varpi_p)$$

where

$$\bar{\epsilon} = |\delta_{1,1}||\delta_{1,0}|^{-4/3}|a|^{1/3}$$
$$\bar{c} = c|\delta_{1,0}|^{-2/3}|a|^{-1/3}\text{sign}(a). \qquad (17)$$

The coefficients that can be adjusted are the width of the second resonance compared to the first (set by $\bar{\epsilon}$) and the separation between the two resonances (set by $\bar{c}$). Variation in $\dot{\varpi}_p$ can be absorbed into our coefficient $\bar{c}$. The term proportional to $\cos(\psi - \varpi)$ is often called the e-resonance since $\Gamma^{1/2} \propto e$. The other term can be called an e'-resonance or a corotation resonance since it does not depend on the particle's longitude of perihelion or ϖ.

Because the corotation resonance does not depend on $\bar{\Gamma}$, it does not grow in volume as the planet migrates. Had we allowed α to depend upon time, the resonance width would grow slightly but not significantly as the planet migrates. Because the resonance volume in phase space does not grow as the planet migrates, this resonance should not capture particles (Yoder 1979). However when this resonance overlaps the other, the system can exhibit large scale chaotic behavior (Holman & Murray 1996). Hence the coupling of the two resonant terms may influence the probability of capture into the e-resonance.

We now ask: *what is the capture probability of the above Hamiltonian as a function of drift rate, $\frac{d\bar{b}}{d\tau}$, and secondary perturbation strength, $\bar{\epsilon}$?* To answer this question we numerically integrate Equation (16), for different parameters $\frac{d\bar{b}}{d\tau}$, and $\bar{\epsilon}$. In this section we work in the limit of low initial particle momentum. This ensures that the probability of capture is 1 in the adiabatic limit and that the transition between capture and no capture would be a sharp transition of drift rate in the case of a single resonance.

Our procedure for numerical integration is the same as described in the previous section. Initial angles are randomly chosen. Initial momenta $(\bar{\Lambda}, \bar{\Gamma})$ are set to small values to ensure a sharp transition when $\bar{\epsilon} = 0$ and the initial momentum are small. The parameter $\bar{b}$ is initially chosen to be ~ -15. For each value of $\frac{d\bar{b}}{d\tau}$ and $\bar{\epsilon}$ we integrated the system 100 times to estimate a resonant capture probability. After the system captures, the momenta variables increase with time and the resonant angle $\phi = \psi - \varpi$ librates about a fixed value. If no capture takes place, the momenta jump as the system pass through resonance.

The coupled two dimensional system exhibits different dynamics than the one-dimensional system considered in the previous section. For example, the resonance can capture for a short period of time, a trajectory we refer to as a temporary capture. An example of a simulation that illustrates a temporary capture is shown in Figure 6. We find that temporary captures tend to occur for larger values of $\bar{\epsilon}$ and drift rate. Quillen (2001) previously showed that temporary capture was exhibited by overlapped resonances using a similar drifting Hamiltonian model.

During a temporary capture, the momenta increase. This also happens if the particle is captured. As in the previous section, we identify a capture if the momentum at the end of the integration exceeds a value of 5. However we then reclassify the integration as a temporary capture if the momenta lie below that expected from a particle still in resonance. These two situations can be differentiated because a particle in resonance has momentum proportional to the time since capture. Temporary captures are excluded when we calculate the capture probability. However, had we integrated the systems longer, it is possible that a particle identified on a short timescale as captured would later drop out of resonance. In other words the precise fraction of captures is dependent on the timescale over which we have integrated these systems and the value of momentum that we have used as a limit to identify captures. This makes our capture probability numerical measurements uncertain primarily at high values of drift rate $|\frac{d\bar{b}}{d\tau}| \gtrsim 1$, and large secondary perturbation strength $\bar{\epsilon} \gtrsim 1$, the regime where we have found temporary captures to be more common.

In Fig. 7 we show a contour plot of the resonant capture probability for $k = 1$, initial $\bar{\Gamma}(t_0) = 10^{-4}$ and resonance separation $\bar{c} = 0$. For high values of the drift rate and low values of the secondary perturbation, $\bar{\epsilon}$, (on lower right in these contour plots) the transition between capture and no capture is sharp and happens at the critical drift rate measured in the previous section. However for lower drift rates and higher values of $\bar{\epsilon}$ the resonance fails to capture for $\bar{\epsilon} \gtrsim 1$. For low drift rates, the transition between capture and no capture is also sharp, but is a function of $\bar{\epsilon}$ instead of drift rate. There are two regimes, that where the drift is so fast that it fails to capture, and that where the corotation resonance is so large that it prevents capture.

For first order resonances we consider the possibility that $\bar{\epsilon}$ could be of order 1. Since $\bar{\epsilon} \propto |\delta_{1,0}|^{-4/3}$, $|\delta_{1,0}| \propto \mu$ and $|\delta_{1,0}| \propto \mu e_p$, the coefficient $\bar{\epsilon} \propto \mu^{-1/3} e_p$. For small planet mass μ we see that the rescaled secondary perturbation strength could be high even at moderate planet eccentricity e_p. The coefficient $\bar{\epsilon}$ could be of order 1 particularly if the planet eccentricity is moderate.

Why is it that for $\bar{\epsilon} \gtrsim 1$ the e-resonance fails to capture particles? A possible explanation is that an increase in $\bar{\Gamma}$ caused by the corotation reduces the capture probability, in the same way that an increase in the initial momentum value does. We would expect that an increase of initial momentum of size ~ 1 caused by the corotation resonance when $\bar{\epsilon} \sim 1$ would strongly reduce the capture probability. This is consistent with the limiting value of $\bar{\epsilon} \lesssim 1$ for capture. This qualitative explanation is also consistent with the lack of dependence of the critical value of $\bar{\epsilon}$ on drift rate (see Figure 7) at drift rates $\left|\frac{d\bar{b}}{d\tau}\right| < 1$. We suspect that the corotation resonance prevents capture into the e-resonance because the corotation resonance raises the particle eccentricity during the resonance encounter. If this were true, then we would

expect that the capture probability would be influenced by the resonance separation. Up to this point we have only considered resonances with separation $\bar{c} = 0$.

4.0.1. *Separated first order resonances*

To further explore the role of multiple resonant terms, we consider the situation when the resonance separation is non zero ($\bar{c}$ not small). The order that the subresonances are encountered as the system drifts can be determined by considering the two resonant angles $\psi - \varpi$ and $\psi - \varpi_p$. The time derivative $\dot{\psi} - \dot{\varpi} = jn - (j-1)n_p - \dot{\varpi}$. As the planet migrates outward n_p drops. For $\dot{\varpi} > \dot{\varpi}_p$ the time derivative of the corotation resonant angle crosses zero first. For $\bar{c} > 0$ (corresponding to $c < 0$ and a positive precession rate for the longitude of periapse), the corotation resonance is encountered first by a particle exterior to a planet as the planet migrates outward. This is what is expected for external resonances in a single planet system where the precession rate of the planet's longitude of periapse $\dot{\varpi}_p = 0$ and $\dot{\varpi} > 0$ due to secular precession induced by the planet.

We consider which resonance is encountered first for other drifting systems. Dust particles migrating inward and exterior to a planet would encounter the resonances in the same order, corotation resonance first as long as $\dot{\varpi} > \dot{\varpi}_p$. Here n is increasing, whereas for the planet migrating outward n_p was decreasing. A particle located internal to a planet that is migrating inward would also encounter the resonances in the same order when $\dot{\varpi} > \dot{\varpi}_p$; (in this case one considers $(j+1)n_p - jn - \dot{\varpi}$ and $(j+1)n_p - jn - \dot{\varpi}_p$ with n_p increasing).

We can compare the width of the corotation resonance to the separation between them. For the e-resonance, the libration width in $\bar{\Lambda}$ depends on the particle eccentricity or $\bar{\Gamma}$. However since the corotation term does not depend on $\bar{\Gamma}$, the corotation resonance width can more easily be estimated as $\Delta\bar{\Lambda} \sim \sqrt{\bar{\epsilon}}$. For

$$|\bar{c}| \lesssim \sqrt{\bar{\epsilon}},$$

the two resonances must overlap. Since $\bar{c} \propto \mu$ and $\sqrt{\bar{\epsilon}} \propto e_p^{1/2}\mu^{-1/6}$, strong resonances are likely to overlap for small planet masses unless the planet eccentricity is extremely small. Because the two resonant terms differ in sign, they have fixed points at different angles, and they are expected to interfere when overlapped even only slightly separated.

We have found that a nonzero value of $\bar{c}$ does change the probability of capture. Figure 8 shows numerical measurements similar to that of Figure 7 but for $\bar{c} = \pm 0.1$. For $\bar{c} < 0$ (Figure 8a) the corotation resonance is encountered after the e-resonance. The onset of the corotation resonance can knock the particle out of resonance, following capture into the e-resonance. For $\bar{c} > 0$ the corotation resonance is encountered first as the planet migrates (Figure 8b). The capture probabilities are primarily modified at low drift rates where higher values of $\bar{\epsilon}$ are required to reduce the probability of capture. It is not obvious why this is the case. From individual integrations we note that the frequency $\bar{c}$ sets an oscillation period that is longer for smaller values of $\bar{c}$. Holman & Murray (1996) found that $\bar{c}$ sets the Lyapunov time of the resonance. So for an overlapped system we might expect more highly chaotic behavior for larger values of $\bar{c}$, particularly at low drift rates. Oddly higher values of $\bar{c}$ at low drift rates seem to stabilize the system, requiring higher values of the corotation resonance strength to kick the particle out of the e-resonance.

For $\bar{c} < 0$ (as shown in Figure 8b) the corotation resonance is encountered after the e-resonance, consequently the corotation resonance is encountered after the e-resonance captures a particle. If the corotation resonance is strong it can knock the particle out of resonance. For larger separations, $\bar{c} \sim 1$, temporary captures are frequent at large $\bar{\epsilon}$. The extended low probability contours on the top end of Figure 8b are in part due to temporary captures.

4.1. *Second order resonances*

When the resonance is second order it contains three subterms (see Equation 3). The first term $\propto \Gamma\cos(\psi - 2\varpi)$ and can be called (e.g., Murray & Dermott 1999) the e^2-resonance since $\Gamma \propto e^2$ at low eccentricity. The second term $\propto e_p\Gamma^{1/2}\cos(\psi - \varpi - \varpi_p)$ and can be called an ee'-resonance. The third term $\propto e_p^2\cos(\psi - 2\varpi_p)$ can be called a corotation or e'^2 resonance. Since the corotation term does not depend on Γ, its volume in phase space does not grow as the planet drifts and it should not be able to capture particles. However, as was true for the first order resonance, this resonant term can prevent the other resonant terms from capturing particles. When the corotation term is not large, both the e^2- and ee'-resonances can capture particles. Since it is $\propto \Gamma^{1/2}$, the ee' term behaves like a first order resonant term, whereas the e^2 term, $\propto \Gamma$, is a second order term. In the previous section we found that first order resonances captured at a somewhat higher drift rate than the second order term and did not require as low initial momenta to exhibit a sharp transition between capture and no capture. The critical drift rate for first order terms is $\propto \mu^{4/3}$ and for second order terms $\propto \mu^2$, a much steeper function of planet mass. Consequently it is possible that the ee' resonant term will capture particles and the e^2-resonance will not capture particles even when the planet eccentricity is low.

We first consider the situation where the e^2-resonance is dominant. Taking $k = 2$ terms from Equation (3), we rescale the Hamiltonian as follows,

$$\begin{aligned}\bar{K}_\xi\bar{\Lambda}, \psi; \bar{\Gamma}, \gamma) = {} & \bar{\Lambda}^2 + \bar{b}_\xi\bar{\Lambda} + \bar{c}_\xi\bar{\Gamma} + \bar{\Gamma}\cos(\psi - 2\varpi) \\ & -\bar{\xi}\bar{\Gamma}^{1/2}\cos(\psi - \varpi - \varpi_p) + \bar{\epsilon}_\xi\cos(\psi - 2\varpi_p)\end{aligned} \tag{18}$$

where

$$\begin{aligned}\bar{\Gamma} &= \left|\frac{\delta_{2,0}}{a}\right|^{-1}\Gamma \\ \tau &= |\delta_{2,0}|t \\ \bar{c}_\xi &= c|\delta_{2,0}|^{-1}\mathrm{sign}(a) \\ \bar{b}_\xi &= b|\delta_{2,0}|^{-1}\mathrm{sign}(a) \\ \bar{\xi} &= |\delta_{2,1}||\delta_{2,0}|^{-3/2}|a|^{1/2} \\ \bar{\epsilon}_\xi &= |\delta_{2,2}||\delta_{2,0}|^{-2}|a|.\end{aligned}$$

The coefficients that can be adjusted are the strength of the ee'-resonance (set by $\bar{\xi}$), the strength of the corotation resonance (set by $\bar{\epsilon}_\xi$), and the separation between the resonances (set by $\bar{c}_\xi$). Since the precession rate

$c \propto \mu$ and the perturbation strength $\delta_{2,0} \propto \mu$ we find that the resonance separation ($\bar{c}$) does not depend on the planet mass. This implies that the subterms could be well separated. This is different than the first order resonances that have $\bar{c} \propto \mu^{1/3}$, which implies that the resonance subterms are often overlapped.

The ee'-resonance strength $\bar{\xi} \propto \mu^{-1/2} e_p$. Since this depends on a negative power of μ, at low planet masses and at high planet eccentricities it is possible that $\bar{\xi} > 1$. In this case the ee'-resonance could be dominant, and we would rescale momentum and time as we did for a first order resonance. In this case we could work with the Hamiltonian (equivalent to the previous one except for the rescaling)

$$\begin{aligned}\bar{K}_\chi(\bar{\Lambda}, \psi; \bar{\Gamma}, \gamma) = &\bar{\Lambda}^2 + \bar{b}_\chi \bar{\Lambda} + \bar{c}_\chi \bar{\Gamma} \\ &+ \bar{\Gamma}^{1/2} \cos(\psi - \varpi - \varpi_p) \\ &- \bar{\chi} \bar{\Gamma} \cos(\psi - 2\varpi) + \bar{\epsilon}_\chi \cos(\psi - 2\varpi_p)\end{aligned} \tag{19}$$

where

$$\begin{aligned}\bar{\Gamma} &= \left|\frac{\delta_{2,1}}{a}\right|^{-2/3} \Gamma \\ \tau &= |\delta_{2,1}|^{2/3} |a|^{1/3} t \\ \bar{b}_\chi &= b |\delta_{2,1}|^{-2/3} |a|^{-1/3} \text{sign}(a) \\ \bar{c}_\chi &= c |\delta_{2,1}|^{-2/3} |a|^{-1/3} \text{sign}(a) \\ \bar{\chi} &= |\delta_{2,0}||\delta_{2,1}|^{-2/3} |a|^{-1/3} \\ \bar{\epsilon}_\chi &= |\delta_{2,2}||\delta_{2,1}|^{-4/3} |a|^{1/3}.\end{aligned} \tag{20}$$

A comparison between Equation (19) and Equation (20) shows that

$$\bar{\xi}^2 = \bar{\chi}^{-3} \tag{21}$$

We suspect that the e^2-resonance is more likely to capture when $\bar{\xi}$ reaches a transitional value that we denote $\bar{\xi}_{trans}$. The ee'-resonance may be more important when $\bar{\chi} \lesssim \bar{\xi}_{trans}^{-2/3}$. If $\bar{\xi} \lesssim \bar{\xi}_{trans}$ then we expect second order behavior ($\dot{n}_{p,crit} \propto \mu^2$) otherwise we expect first order behavior ($\dot{n}_{p,crit} \propto \mu^{4/3}$). We note that the order the resonances are encountered is also important. Here we numerically measure a capture probability that does not specify which resonance captures. If the drift rate is sufficiently slow that the e^2-resonance captures and this resonance is reached first then this resonance will dominate the capture probability.

As we did for the $k = 1$ resonances we have measured the capture probability for a range of coefficients and drift rates. Figure 9a shows the capture probability for the Hamiltonian of Equation (18) with varying drift rate, and ee'-resonance perturbation strength, $\bar{\xi}$, and with no corotation term; $\bar{\epsilon}_\xi = 0$. The resonances are not separated; $\bar{c}_\xi = 0$. On the lower left side of this plot, for weak $\bar{\xi}$ we see capture behavior consistent with the pure second order ($k = 2$) system discussed in the last section with only one resonant term. With the variables defined in this section (which differ by a factor of $k = 2$ from those defined in Equation 7) $\left|\frac{d\bar{b}}{d\tau}\right|_{crit} = 0.5$. The capture probability ceases to depend on $\bar{\xi}$ for $\bar{\xi} \lesssim 10^{-2}$. Consequently we can estimate a transition value

$$\bar{\xi}_{trans} \sim 10^{-2} \tag{22}$$

valid for low initial particle momentum. For $\bar{\xi} \gtrsim \xi_{trans}$, the transition between capture and no capture occurs at faster drift rates and the transition drift rate is a function of $\bar{\xi}$. For $\bar{\xi} > \bar{\xi}_{trans}$ the system behaves like a first order system, and since the perturbation strength depends on $\bar{\xi}$ we expect the transition drift rate to depend on $\bar{\xi}^{4/3}$. This is consistent with the trend shown on the upper right in Figure 9a. For large $\bar{\xi}$ and at high drift rates the system can fail to capture into the e^2-resonance but can be captured into the ee'-resonance. In short, for $\bar{\xi} \lesssim \bar{\xi}_{trans}$ the system behaves like a second order system and tends to capture into the e^2-resonance, however for $\bar{\xi} \gtrsim \bar{\xi}_{trans}$ the highly overlapped system behaves like a first order system and tends to capture into the ee'-resonance.

Figure 9b shows the capture probability for the Hamiltonian of Equation (19) with varying drift rate, varying e^2-resonance perturbation strength, $\bar{\chi}$ and with no corotation term; $\bar{\epsilon}_\chi = 0$. The resonances are not separated; $\bar{c}_\chi = 0$. This figure extends Figure 9a to $\bar{\xi} > 1$ because $\bar{\chi} = \bar{\xi}^{-2/3}$. At small $\bar{\chi}$ the system critical drift rate is independent of $\bar{\chi}$ and consistent with that measured in section 3 for a first order resonance with $\left|\frac{d\bar{b}}{d\tau}\right|_{crit} = 2$. At this limit the system behaves like a first order resonance. The second order regime is not fully reached until $\bar{\xi} \sim \bar{\xi}_{trans}$ which would correspond to $\bar{\chi} > 20$. However, for large values of $\bar{\xi}$ we see that the critical drift rate does begin to increases, consistent with a dependence of critical drift rate on $\bar{\chi}$ (the second order term dominates). In Figure 9b where $\bar{\chi} \sim 0.5$ we see an extended region of drift rates corresponding to a regime of intermediate capture probability. We have inspected individual integrations from this region and seen temporary captures and widely varying or chaotic trajectories. The intermediate capture probability measured is probably due to interference between the two similarly sized and overlapped e^2- and ee'-resonances.

Figures 9 shows integrations done for low initial particle eccentricity (low $\bar{\Gamma}(t_0)$). We discuss what we expect would happen for higher initial particle momentum. The second order resonance is more strongly affected by the initial particle momentum. For larger $\bar{\Gamma}(t_0)$ the drop in probability at the bottom right on Figure 9a would occur at a faster drift rate and the drop would be smoother. The contours would broaden and shift to the right, primarily on the bottom of Figure 9a. The resonance behaves like a second order resonance at the top right of Figure 9b. So we expect a similar broadening and shifting to the right of the contours at the top of Figure 9b.

We now investigate the role of the corotation or e'^2 resonance term. When the e^2 term is not important (as we have found $\bar{\xi} \gtrsim \bar{\xi}_{trans}$), the system is identical to that studied in the previous section for $k = 1$ with two terms (Equation 16). However we can also study the system for Equation 18 as a function of $\bar{\epsilon}_\xi$ and with $\bar{\xi} = 0$ so the corotation term is strong but the ee'-resonance is weak. Figure 10 shows the capture probability for the Hamiltonian of 18 with varying $\bar{\epsilon}_\xi$ drift rate, $\frac{d\bar{b}}{d\tau}$, and with $\bar{\xi} = \bar{c}_\xi = 0$. We find here that even moderate values of the corotation resonance strength $\bar{\epsilon} \sim 0.1$ can significantly reduce the capture probability. The corotation resonance can reduce the probability of capture for both

first and second order resonances.

4.1.1. *Separated second order resonances*

As was true for the first order resonances we expect the capture probability to depend on the resonant term separations and order that the resonances are encountered. Figure 11 shows the effect of changing the resonance separation $\bar{c}_\xi$ when the e^2-resonance dominates. Figure 11a shows the case with widely separated resonances when the e^2-resonance is encountered first. We see that the transition value of ξ_{trans} is higher than when there is no separation ($\bar{c} = 0$). When the e^2-resonance is encountered afterward the transition value of ξ_{trans} is lower. The ee'-resonance interferes with the capture into the e^2-resonance to a higher degree when this resonance is encountered earlier. Figure 11 shows the effect of changing the resonance separation $\bar{c}_\chi$ when the ee'-resonance dominates. We find that the region of intermediate capture probability at $\bar{\chi} \sim 0.5$ is smaller when the resonances are separated than when $\bar{c} = 0$ (Figure 9b).

5. APPLICATIONS

In this section we apply what we have learned above to two systems involving capture into the 2:1 resonance. When the 2:1 resonance is exterior (and capture particles as a planet migrates outward) the e-resonance strength is reduced because of the indirect term. This reduces the critical migration rate compared to that for other first order resonances. Because the corotation resonance is not affected by the indirect term, it is comparably strong. Consequently even a small planet eccentricity can reduce the capture probability. When the 2:1 resonance is interior (and can capture for a planet migrating inward) the indirect term reduces the strength of the corotation resonance instead of the e-resonance. In this case the 2:1 resonance is strong and can capture at fairly high migration rates. We consider two situations, the capture of twotinos into the 2:1 resonance by Neptune migrating outward, and the capture of an inner extra solar planet into the 2:1 or 3:1 resonance by an inward migrating planet exterior to it.

5.1. *The capture of twotinos in the Kuiper Belt via Neptune's migration*

In this section we consider the capture of Kuiper belt objects into the 2:1 resonance by an outward migrating Neptune. We see from Table 1 that the 2:1 external resonance has exceptionally large values of $\bar{\epsilon}$ compared to the 3:2 and 4:3 resonances. This is because $\delta_{1,0}$ is small due to the addition of the indirect term.

We first consider the critical migration rate allowing capture and compare the one we predict here with that found from numerical studies. Migration rates are often given in terms of the time it takes to cross the range of radius covered during the entire migration. This is typically a few AU for Neptune's migration (Ida et al. 2000; Chiang & Jordan 2002). To compare migration rates to the critical one estimated above, we must first convert rates into our system of units. For $GM_\odot = 1$ and radii in units of Neptune's semi-major axis, a_N, we multiply timescales by $\sqrt{a_N^3/GM_\odot} = 26.1$ years. A migration rate of a few AU in 10^7 years corresponds to $\dot{a}_p \sim 2.6 \times 10^{-7} \left(\frac{10^7 \mathrm{yr}}{t_{migrate}}\right)$. Since $n_p \propto a_p^{-3/2}$ this corresponds to $\dot{n}_p \sim 3.9 \times 10^{-7} \left(\frac{10^7 \mathrm{yr}}{t_{migrate}}\right)$. The critical planet migration rate (listed in Table 1) for Neptune's 2:1 resonance is $\dot{n}_{p,crit} \approx 0.54\mu^{4/3} \approx 1.0 \times 10^{-6}$. We find that

$$\frac{\dot{n}_p}{\dot{n}_{p,crit}} \approx 0.4 \left(\frac{10^7 \mathrm{yr}}{t_{migrate}}\right). \tag{23}$$

Chiang & Jordan (2002) found that 2:1 resonance captured at the 50% level for $t_{migrate} = 10^7$ years but was much less efficient, capturing only 15% of particles at faster migration rates of $t_{migrate} \sim 10^6$ years. The same rise in capture probability at $t_{migrate} \sim 10^7$ years was seen by Ida et al. (2000). The sharp drop in capture probability is consistent with our predicted limit for the critical migration rate. We find that we can account for the trends seen in the numerical studies of Ida et al. (2000); Chiang & Jordan (2002) and confirm the theoretical explanation of Friedland (2001). We note that the transition from a probability of 50% to 15% occurs over a fairly large range of drift rates. In our toy model we could account for such a smooth transition with initial particle eccentricity near e_{lim}. However because the capture probability drops steeply for $e_0 > e_{lim}$ this explanation would require fine tuning of the initial particle eccentricity distribution. We note that it is impossible to zero the eccentricity of a particle in a simulation because of other perturbations. Also, because we have dropped most cosine terms in Equation (3), We have neglected these other perturbations in our Hamiltonian model. Consequently it is difficult for us to compare the initial eccentricity distribution of a simulation to the distribution in our momentum $\bar{\Gamma}$.

We now consider the role of the corotation resonance. From table 1 we find $\bar{\epsilon} = 6.6\mu^{-1/3}e_p$. For Neptune $\mu = 5.1 \times 10^{-5}$ and we find that $\bar{\epsilon} \approx 180e_p$. For Neptune's current eccentricity $e_p \sim 0.008$ this places $\bar{\epsilon} \sim 1.4$. This is somewhat above the critical corotation strength value allowing capture into the 2:1 resonance according to figure 7 when the resonances are on top of each other. We need to consider the separation between the resonances; $\bar{c} = 1.18\mu^{1/3} = 0.04$. However this is the separation only if Neptune's longitude of perihelion does not precess. Neptune's precession frequency is largely due to the solar system's eighth eigenvector that dominates this planet's secular motions (Nobili et al. 1986; Applegate et al. 1986). Neptune's precession rate due to other planets is a few times larger than that it induces on objects in its 2:1 resonance. Consequently $\bar{c}$ could be larger a factor of a few and either positive or negative depending upon the secular motion of the planet when the migration took place. Smaller values of planet eccentricity would allow the 2:1 to capture whereas larger values would tend to make it more difficult. Negative values of $\bar{c}$ would allow the resonance to be in the temporary capture regime shown in Figure 8a whereas positive values of $\bar{c}$ would allow capture at Neptune's current eccentricity, provided the migration was slow (Figure 8b). It is interesting to find that Neptune's eccentricity is very near the critical value that would make this resonance fail to capture. This large value of $\bar{\epsilon}$ could contribute to the intermediate capture probability seen in simulations and the moderate range of drift rates where this intermediate capture occurs.

5.2. *Capture into the 2:1 and 3:1 Resonances of Multiple Extrasolar Planet systems*

Three extrasolar multi-planet systems have two planets locked in the 2:1 resonance, GL876, HD 82943, and HD128311 (Marcy et al. 2005). In each case the outer planet is more massive than the inner one. The masses of the outer planet are 1.9, 1.6 and 3.2 2 M_J (Jupiter masses), respectively. We assume that an outer planet has migrated inward and captured the interior and lower mass planet into the 2:1 resonance (e.g., as explored previously by Kley et al. 2004, 2005; Moorhead & Adams 2005). The coefficients for this situation are listed in the appendix and in Table 1. For an internal 2:1 mean motion resonance $\dot{n}_{p,crit} = 22.7\mu^{4/3}$. We relate the critical mean motion drift rate to a critical semi-major axis drift rate (with a factor of 2/3) and restore the units. To capture an internal planet into the 2:1 resonance a planet must have a migration rate slower than

$$\dot{a}_p \lesssim 15\mu^{4/3}\left(\frac{GM_*}{a_p}\right). \quad (24)$$

Using the period of the planet's orbit, $P = 2\pi\sqrt{\frac{a_p^3}{GM_*}}$, we can relate the critical migration rate to a timescale, $\tau = a_p/\dot{a}_p$, finding

$$\tau_{2:1} \gtrsim 0.4\mu^{-4/3}P \quad (25)$$

for the 2:1 resonance For a $2M_J$ mass planet, we find a migration timescale of longer than 1600 orbital periods is required for the 2:1 resonance to capture. This limit is consistent with the timescales adopted for migration in the simulations by Kley et al. (2004). We can consider the eccentricity limit (taking the value from Table 1) $e_{lim} \sim 1.5\mu^{1/3} = 0.2$. This implies that the initial eccentricity of the inner planet (as long as it was below 0.2) would probably not limit the capture probability into the 2:1 resonance.

We now consider capture into the 3:1 resonance. The 55 CnC system has two planets locked in the 3:1 resonance with outer planet $0.2M_J$ and inner planet with $0.8M_J$. Even though the inner planet is more massive we consider capture into an internal resonance because the 3:1 internal resonance is stronger than the external one. This is a result of the contributions from the indirect terms. Using values given in the appendix in Table 2 for an internal 3:1 resonance we find $\dot{n}_{p,crit} = 0.6\mu^2$ for the e^2 resonance and $\dot{n}_{p,crit} = 41\mu^{4/3}e_p^{4/3}$ for the ee' resonance, in both cases for low initial particle eccentricity. This corresponds to a migration timescale

$$\tau_{3:1,e2} \gtrsim 15\mu^{-2}P \quad (26)$$

for the e^2 resonance and

$$\tau_{3:1,ee'} \gtrsim 0.2\mu^{-4/3}e_p^{-4/3}P \quad (27)$$

for the ee' resonance. However the migration rate is less restrictive for the e^2 resonance if the inner planet has a moderate eccentricity. The limiting eccentricity is $e_{lim} \sim 0.2\mu^{1/2}$. For $\mu = 0.002$, we find $e_{lim} = 0.003$. Consequently the inner planet is likely to have $e > e_{lim}$. In this case the migration timescale must be modified by the factor given in Equation (15) and the limiting migration timescale would be ~ 10 times smaller or

$$\tau_{3:1,ee'} \gtrsim 0.02\mu^{-4/3}e_p^{-4/3}P. \quad (28)$$

For $\mu = 0.0002$ to capture we find the migration timescale must be longer than a few times 10^7 orbits for the e^2 resonance and $20000e_p^{-4/3}$ orbits for the ee' resonance. For a moderate planet eccentricity of 0.2 this corresponds to a timescale of 2×10^5 orbits.

We have found here that capture into the 2:1 resonance by the multiple planet extra solar systems does not require a slow migration rate but capture into the 3:1 resonance does. For the 3:1 resonance faster migrations are allowed for the ee' resonance than the e^2 resonance. The limiting timescale is decreased if the planet eccentricities are not low prior to resonance capture.

6. SUMMARY AND DISCUSSION

In this paper we have explored the problem of resonance capture for mean motion resonances at fast or non-adiabatic drift rates. We first studied the first and second order time dependent Hamiltonian system with one resonant term. We find that for sufficiently low initial particle momentum (or eccentricity), the transition between resonance capture and no capture is sharp, occurring over a narrow range in drift rate. We give an expression (Equation 14) which makes it possible to predict the critical planetary migration rate (above which there is no capture) for first and second order mean motion resonances in the general restricted three body problem in the limit of low initial particle eccentricity. Expressions are given in the appendix for coefficients which allow one to estimate the critical drift rate for any first or second order mean motion resonance. Coefficients are evaluated for strong resonances and listed in Tables 1 and 2. This generalizes upon previous analytical work by Friedland (2001) and provides a theoretical explanation for critical drift rates measured numerically and their dependence on planet mass (e.g., Ida et al. 2000; Wyatt 2003).

We have numerically measured the probability of capture as a function of initial particle eccentricity. We find that the transition between resonance capture and no capture is smoother, occurring over a larger range in drift rate, for initial particle eccentricity of order the limiting value ensuring capture in the adiabatic limit, e_{lim}. The drift rate at which the capture probability is half is not strongly dependent on the initial particle eccentricity for first order resonances, and the probability of capture drops rapidly for initial particle eccentricities exceeding the limiting value, e_{lim}. For second order resonances, we find that the drift rate at which the capture probability is half is higher when the initial particle eccentricity is higher. Equation (15) can be used to estimate the half probability drift rate for initial eccentricities below $10e_{lim}$. At $e_0 \gtrsim 30e_{lim}$ the capture probability drops below 1/2 at all drift rates.

In the limit of low initial particle eccentricity, we have considered the case of resonances containing multiple subterms. A first order resonance fails to capture when the corotation resonance has unitless strength $\bar{\epsilon} \gtrsim 1$. As this coefficient depends on planet eccentricity, migrating, eccentric, low mass planets could have first order resonances that fail to capture particles for this reason. A regime of intermediate capture probability also exists at high drift rates and large corotation perturbation strength. We have found that the resonance separation, and order of encounter, affects the capture probability, primarily when the corotation resonance is strong. This

implies that the capture probability is dependent upon the precession rates of the longitude of periapse of both particle and planet.

Second order resonances contain three subterms. As was true for the first order resonances, the corotation resonance fails to capture particles but can prevent the other resonant terms from capturing particles if scale free parameters $\bar{\epsilon}_\xi \gtrsim 1$ or $\bar{\epsilon}_\chi \gtrsim 1$. This implies that above a certain planet eccentricity, second order resonances fail to capture particles. Below this planet eccentricity the e^2- and ee'-resonances can capture particles. When our coefficient $\bar{\xi} \lesssim 10^{-2}$ the e^2-resonance will capture particles (providing the drift rate is sufficiently slow) and the capture behavior is second order. For $\bar{\chi} < 0.1$ the ee'-resonance will capture particles and the behavior is first order. For nonzero planet eccentricity, the ee' subresonance (which behaves like a first order resonance) may more easily capture particles at faster drift rates than the e^2 resonance. For $\bar{\chi}$ or $\bar{\xi}$ of order 1, a regime of intermediate capture probability exists at high drift rates. For second order resonances the subresonance separation, and order of encounter also affects the capture probability.

A number of effects have been proposed to account for reduction in capture probabilities compared to those predicted via adiabatic theory, e.g., Zhou et al. (2002) showed that stochastic or jumpy migration would allow particles to escape resonances. Here we have shown that rich dynamics in the non-adiabatic limit allows particles to escape resonance capture. We have shown that corotation terms can reduce the capture probability. For second order resonances, resonant subterms can interfere, again producing a regime of intermediate capture probability. For first order resonances, the half probability drift rates are not strongly dependent on the initial particle eccentricity, and the probability of capture drops rapidly above a limiting initial eccentricity. However for second order resonances the half probability drift rate is higher for initial particle eccentricity near the limiting value. Consequently we expect that second order resonances should have larger regimes of intermediate capture probability in range of drift rate and initial particle eccentricity.

We have applied our understanding to the problem of capturing twotinos via Neptune's migration. We find that the eccentricity of Neptune is sufficiently high that the 2:1 resonance could fail to capture particles. Certainly if Neptune's eccentricity were any higher during migration its 2:1 resonance would not have captured particles efficiently. It is interesting to find that Neptune's eccentricity is very near the critical value that would make this resonance fail to capture particles.

We have applied our framework toward predicting mininum migration timescales allowing extra solar multiple planet systems to capture into the 2:1 or 3:1 resonances. We find that a migration timescale of greater than a few thousand orbital periods is required to allow capture into the 2:1 resonance for three systems. However a much longer timescale, $\sim 10^7$, orbital periods is required to allow capture into the 3:1 resonance for the 55 Cnc planetary system. The migration timescale can be somewhat reduced if the planets are on moderately eccentric orbits subsequent to migration.

In this work we have extended the theory of resonant capture for drifting Hamiltonian systems to the non-adiabatic limit and to systems with multiple resonant subterms. We have provided a theoretical framework to predict resonance capture probabilities. However this framework is based on numerical integration of a simplistic two-dimensional Hamiltonian model and so may not accurately represent the full complex dynamical systems. Direct numerical integration of these systems must be carried out to test the validity and accuracy of the expressions given in this paper. The exploration done here could also in future be extended via numerical study of modified quasi Hamiltonian toy models (e.g., Gomes (1997)) to better cover systems with drift induced by non-conservative forces such as gas drag or Poynting-Robertson drag. This work could also be extended to cover motions out of the plane and high eccentricity systems.

I thank the Research School of Astronomy and Astrophysics of the Australian National University and Mount Stromlo Observatory for hospitality and support during Spring 2005. Support for this work was in part provided by National Science Foundation grant AST-0406823, and the National Aeronautics and Space Administration under Grant No. NNG04GM12G issued through the Origins of Solar Systems Program. Support was also provided by the National Science Foundation to the Kavli Institute for Theoretical Physics under Grant No. PHY99-07949.

APPENDIX

COEFFICIENTS FOR INTERNAL AND EXTERNAL RESONANCES

External resonances

For external first order resonances,

$$K(\Lambda,\psi;\Gamma,\gamma) = a\Lambda^2 + b\Lambda + c\Gamma + \delta_{1,0}\Gamma^{1/2}\cos(\psi-\varpi) + \delta_{1,1}\cos(\psi-\varpi_p) \quad \text{(A1)}$$

with

$$\delta_{1,0} = -\mu\sqrt{2}\alpha^{5/4} f_{31}$$
$$\delta_{1,1} = -\mu e_p \alpha f_{27}. \quad \text{(A2)}$$

Coefficients a, b, and c are given in Equations (2) and (4). The f_i are functions of the Laplace coefficients and are evaluated at α with index j using expressions from the appendix by Murray & Dermott (1999).

The above expressions only include direct terms. For the 2:1 resonance the indirect term contributes and

$$\delta_{1,0}(2:1) = -\mu\sqrt{2}\alpha^{1/4}\left(\alpha f_{31} - \frac{1}{2\alpha}\right) \quad \text{(A3)}$$

The near cancellation of the direct and indirect terms makes second order terms important for the 2:1 resonance (Friedland 2001; Murray-Clay & Chiang 2005). It may be useful to recall the maximum initial particle momentum or initial eccentricity, e_{lim} ensuring capture in the adiabatic limit. This corresponds to

$$e_{lim} = \sqrt{2\bar{\Gamma}_{0,lim}}\alpha^{1/4}\left|\frac{\delta_{1,0}}{a}\right|^{1/3} \tag{A4}$$

where $\bar{\Gamma}_{0,lim} = 3/2$.

For external second order resonances or $k = 2$,

$$\begin{aligned} K(\Lambda,\psi;\Gamma,\gamma) = & a\Lambda^2 + b\Lambda + c\Gamma \\ & +\delta_{2,0}\Gamma\cos(\psi - 2\varpi) \\ & +\delta_{2,1}\Gamma^{1/2}\cos(\psi - \varpi - \varpi_p) \\ & +\delta_{2,2}\cos(\psi - 2\varpi_p) \end{aligned} \tag{A5}$$

where

$$\begin{aligned} \delta_{2,0} &= -\mu 2\alpha^{3/2} f_{53} \\ \delta_{2,1} &= -\mu e_p\sqrt{2}\alpha^{5/4} f_{49} \\ \delta_{2,2} &= -\mu e_p^2\alpha f_{45}. \end{aligned} \tag{A6}$$

Coefficients a, b and c are given in Equations (2) and (4). For the 3:1 resonance the indirect term contributes and

$$\delta_{2,0}(3:1) = -\mu 2\alpha^{1/2}\left(\alpha f_{53} - \frac{3}{8\alpha}\right). \tag{A7}$$

For second order resonances capturing into the e^2 subterm

$$e_{lim,\xi} = \sqrt{2\bar{\Gamma}_{0,lim}}\alpha^{1/4}\left|\frac{\delta_{2,0}}{a}\right|^{1/2} \tag{A8}$$

where the critical scale free momentum $\bar{\Gamma}_{0,lim} = 1/8$. For those capturing into the ee' subterm

$$e_{lim,\chi} = \sqrt{2\bar{\Gamma}_{0,lim}}\alpha^{1/4}\left|\frac{\delta_{2,1}}{a}\right|^{1/3} \tag{A9}$$

where the critical scale free momentum $\bar{\Gamma}_{0,lim} = 3/2$.

Internal resonances

To make our theory appropriate for internal resonances (external perturber) we would consider $j : j + k$ resonances and change the coefficients to

$$\begin{aligned} a &= -\frac{3}{2}j^2\alpha^{-2} \\ b &= -(j+k)(n_p - 1) \\ c &= -\mu 2 f_2\alpha^{-1/2} \\ \delta_{1,0} &= -\mu\sqrt{2}\alpha^{-1/4} f_{27} \\ \delta_{1,1} &= -\mu e_p f_{31} \\ \delta_{2,0} &= -\mu 2\alpha^{-1/2} f_{45} \\ \delta_{2,1} &= -\mu e_p\sqrt{2}\alpha^{-1/4} f_{49} \\ \delta_{2,2} &= -\mu e_p^2 f_{53} \end{aligned} \tag{A10}$$

where $\alpha \equiv a/a_p$ and we have used the approximation $e^2 \sim 2\Gamma/L \sim 2\Gamma\alpha^{-1/2}$. The c term describes secular precession of the longitude of periapse and depends on the function f_2 given in the appendix by Murray & Dermott (1999) and is evaluated at α with index $j = 0$. For internal resonances the other f_i functions are evaluated at α with index $j + k$ using expressions from the appendix by Murray & Dermott (1999). For the 2:1 and 3:1 resonances the indirect terms contribute and

$$\delta_{1,1}(2:1) = -\mu e_p\left(f_{31} - 2\alpha\right) \tag{A11}$$

$$\delta_{2,2}(3:1) = -\mu e_p^2\left(f_{53} - \frac{27}{8}\alpha\right). \tag{A12}$$

The maximum initial particle eccentricity ensuring capture in the adiabatic limit for first order resonances

$$e_{lim} = \sqrt{2\bar{\Gamma}_{0,lim}}\alpha^{-1/4}\left|\frac{\delta_{1,0}}{a}\right|^{1/3} \tag{A13}$$

where $\bar{\Gamma}_{0,lim} = 3/2$. For second order resonances capturing into the e^2 subterm

$$e_{lim,\xi} = \sqrt{2\bar{\Gamma}_{0,lim}}\alpha^{-1/4}\left|\frac{\delta_{2,0}}{a}\right|^{1/2} \tag{A14}$$

where the critical scale free momentum $\bar{\Gamma}_{0,lim} = 1/8$. For those capturing into the ee' subterm

$$e_{lim,\chi} = \sqrt{2\bar{\Gamma}_{0,lim}}\alpha^{-1/4}\left|\frac{\delta_{2,1}}{a}\right|^{1/3} \tag{A15}$$

where the critical scale free momentum $\bar{\Gamma}_{0,lim} = 3/2$. The drift rate for a capture probability of $1/2$ given in Equation (15) must be modified for second order internal resonances;

$$|\dot{n}_{p,1/2}| \sim 0.5(j-2)\delta_{2,0}^2\left(1 + \frac{\alpha^{1/2}e_0^2 a}{2.4\times 10^{-4}\delta_{2,0}}\right)^{0.25}. \tag{A16}$$

This expression is valid for initial particle eccentricity $e_0 \lesssim 10e_{lim,\xi}$.

The coefficients for strong internal and external resonances are listed in Tables 1 and 2.

MIGRATION OF DUST VIA POYNTING-ROBERTSON DRAG

In this paper we have considered an varying Hamiltonian system. However there may be some similarities between this system and the slowly drifting dissipative systems. We add relations that allow the reader to approximately predict the critical drift rates for dust spiraling inward under Poynting-Robertson drag. In the case of Poynting Robertson drag dust particles in a circular orbit decay on a timescale proportional β^{-1} where β is the ratio of radiation to gravitational (from the star) forces. It is convenient to write

$$\beta \sim \frac{0.2}{s_{\mu m}}\left(\frac{L_*}{L_\odot}\right)\left(\frac{M_*}{M_\odot}\right)^{-1} \tag{B1}$$

where $s_{\mu m}$ is the radius of the particle in μm and L_* is the luminosity of the star (Sicardy et al. 1993). The drag force leads to a slow increase in the mean motion

$$\dot{n} \sim \frac{3\alpha^{1/2}\beta}{c_l} \tag{B2}$$

where c_l is the speed of light in units of the planet's velocity or divided by $\sqrt{GM_*/a_p}$. The value of our coefficient b is not important, as long as it passes through zero on resonance. However, its drift rate or $\dot{b}$ is important. At resonance $jn = (j-k)n_p$ and we can relate the drift rate of the particle spiraling inward to a system of a planet migrating outward considered in the previous sections. We replace $\dot{n}_p$ with $\dot{n}$, finding an effective drift coefficient

$$\dot{b} = \frac{3j\alpha^{1/2}\beta}{c_l}. \tag{B3}$$

The rescaled speed of light

$$c_l \approx 10^4\left(\frac{M_*}{M_\odot}\right)^{-1/2}\left(\frac{a_p}{1AU}\right)^{1/2}. \tag{B4}$$

Consequently we can write

$$\dot{b} = 0.6\times 10^{-4} j\alpha^{1/2}s_{\mu m}^{-1}\left(\frac{L_*}{L_\odot}\right)\left(\frac{M_*}{M_\odot}\right)^{-1/2}\left(\frac{a_p}{1AU}\right)^{-1/2}. \tag{B5}$$

The above relation can be used to approximately determine the minimum size particles that can be captured into resonances using the formulation presented in previous sections of this paper.

REFERENCES

Applegate, J. H., Douglas, M. R., Gursel, Y., Sussman, G. J., & Wisdom, J. 1986 , AJ, 92, 176

Borderies, N., & Goldreich, P. 1984, Celestial Mechanics, 32, 127

Chiang, E. I., & Jordan, A. B. 2002AJ, 124, 3430

Deller, A. T., & Maddison, S. T. 2005, ApJ, 625, 398

Dermott, S. F., Jayaraman, S., Xu, Y. L., Gustafson, B. A. S., & Liou, J. C. 1994, Nature, 369, 719

Dermott, S.F., Malhotra, R., & Murray, C. D. 1988, Icarus, 76, 925

Fernandez, J. A., Ip, W.-H. 1984, Icarus, 58, 109

Gomes, R. S. 1995, Celestial Mechanics and Dynamical Astronomy, 61, 97

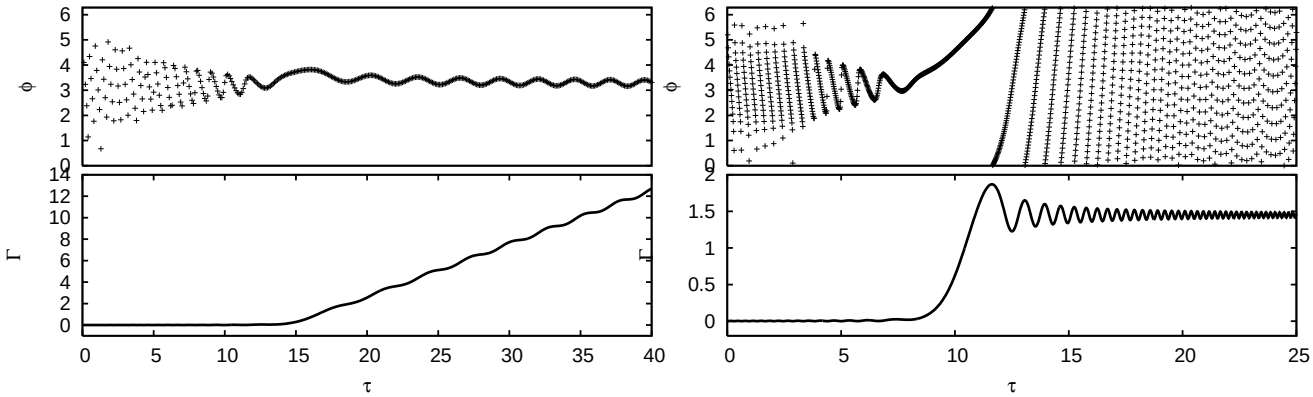

FIG. 1.— a) This integration shows a resonant capture. We show different behavior for the drifting system with one resonant term, Equation (8), as it passes through resonance. For these integrations the resonance is first order ($k = 1$), and the initial momentum $\bar{\Gamma}(t_0) = 10^{-4}$. The solid lines shows $\bar{\Gamma}$. The dots show the resonant angle ϕ. After capture at a time $\tau \sim 15$, the resonant angle librates about π and the momentum $\bar{\Gamma}$ slowly increases. The rate of increase is set by the drift rate; for this integration is $\frac{d\bar{b}}{d\tau} = 1$. b) No capture takes place in this integration which has a higher drift rate of $\frac{d\bar{b}}{d\tau} = 2.3$. The resonant angle ϕ circulates during the entire integration. The momentum oscillates about a fixed value before and after resonance. There is an increase or jump in the mean momentum as the system passes through resonance at $\tau \sim 10$.

Gomes, R. S. 1997, A& A, 321, 967
Friedland, L. 2001, ApJ, 547, L75
Hahn, J. M., & Malhotra, R. 1999, AJ, 117, 3041
Hahn, J. M., & and Malhotra, R. 2005, AJ, in press
Henrard, J. 1982, Celestial Mechanics, 27, 3
Henrard, J. & Lemaitre, A. 1983, Celestial Mechanics, 30, 197
Holman, M. J., & Murray, N. W. 1996, AJ, 112, 1278
Ida, S., Bryden, G., Lin, D. N. C.; & Tanaka, H 2000, ApJ, 534, 428
Kley, W., Lee, M.-H., Murray, N., Peale, S. 2005, A&A, in press, astro-ph/0503579
Kley, W., Peitz, J., & Bryden, G. 2004, A&A, 414, 735
Levison, H. F., Morbidelli, A. 2003, Nature, 426, 419
Liou, J.-C., & Zook, H. A. 1997, Icarus, 128, 354
Liou, J.-C., & Zook, H. A. 1999, Icarus, 118, 580
Malhotra, R. 1990, Icarus, 87, 249
Malhotra, R. 1995, AJ, 110, 420
Marcy, G., Butler, R. P., Fischer, D. A., Vogt, S. S., Wright, J. T., Tinney, C. G., & Jones, H. R. A. 2005, astro-ph/0505003
Marzari, F., & Vanzini, V. 1994, A&A, 283, 275
Moorhead, A. V., & Adams, F. C. 2005, Icarus in press, (astro-ph/0505234)
Moro-Martin, A., Wolf, S., & Malhotra, R. 2005, ApJ, 621, 1079
Murray, C. D. & Dermott, S. F. 1999, Solar System Dynamics, Cambridge University Press, Cambridge
Murray-Clay, R. A., & Chiang, E. I. 2005, ApJ, 619, 623
Nobili, A. M., Milani, A., & Carpino, M. 1989, A&A, 210, 313
Ozernoy, L. M., Gorkavyi, N. N., Mather, J. C.,& Taidakova, T. A. 2000, ApJ, 537, L147
Peale, S.J. 1986 in Satellites edited by Burns, J.A., & Matthews M.S., Univ. of Arizona Press, p 159
Quillen, A. C., Holman, M 2000, AJ, 119, 397
Quillen, A. C. 2001, (astro-ph/0012466)
Sicardy, B., Beauge, C., Ferraz-Mello, S., Lazzaro, D., & Roques, F. 1993, Celestial Mechanics and Dynamical Astronomy, 57, 373
Tittemore, W. C., & Wisdom, J. 1990, Icarus, 85, 394
Wilner, D. J., Holman, M. J., Kuchner, M. J., & Ho, P. T. P. 2002, ApJ, 569, L115
Wyatt, M. C. 2003, 598, 1321
Wisdom, J. 1980, AJ, 85, 1122
Yoder, C. 1979, Celest. Mech., 19, 3
Zhou, L.-Y., Sun, Y.-S., Zhou, J.-L., Zheng, J.-Q., & Valtonen, M. 2002, MNRAS, 336, 520

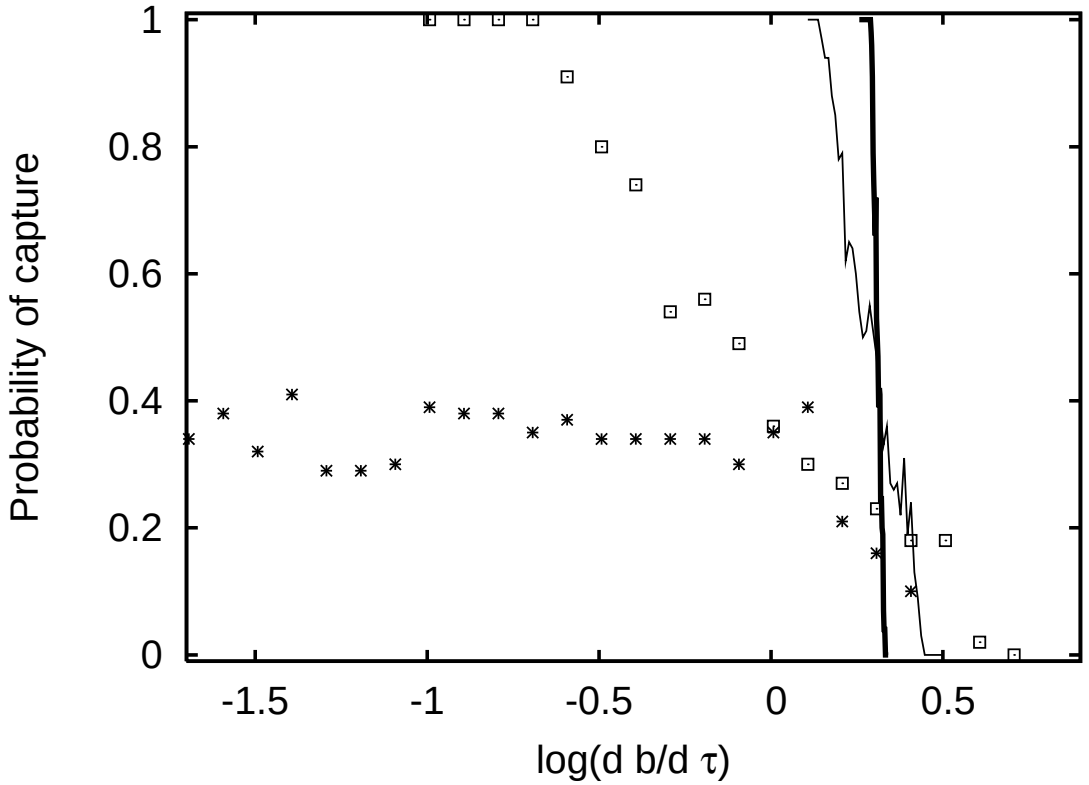

FIG. 2.— Capture probabilities for a Hamiltonian system Equation (8) with one first order ($k = 1$) resonant term as a function of drift rate $\left|\frac{d\bar{b}}{d\tau}\right|$ and initial momentum $\bar{\Gamma}(t_0)$. Note that low $\bar{\Gamma}(t_0)$ corresponds to low initial eccentricity. The thick and thin solid lines shows the capture probability for $\bar{\Gamma}(t_0) = 10^{-4}$ and 10^{-1} respectively. The squares and stars show the capture probability for $\bar{\Gamma}(t_0) = 1$ and 2.3 respectively. In the adiabatic limit for $\bar{\Gamma}(t_0) < 1.5$ the capture probability is 1. For $\bar{\Gamma}(t_0) = 2.3$ the capture probability is intermediate for low drift rates and approaches a constant value as the system becomes more adiabatic. For initial momentum low (10^{-4}) the transition between 100% capture and 0% capture is extremely sharp. We find that if the initial momentum is ~ 1 then there is a regime or a range of drift rates where the capture probability is intermediate. With a change of scale, all first order resonances can be put in the form of Equation (8). Consequently the probabilities shown here can be used to estimate the capture probability in the non-adiabatic limit for any migrating first order resonance.

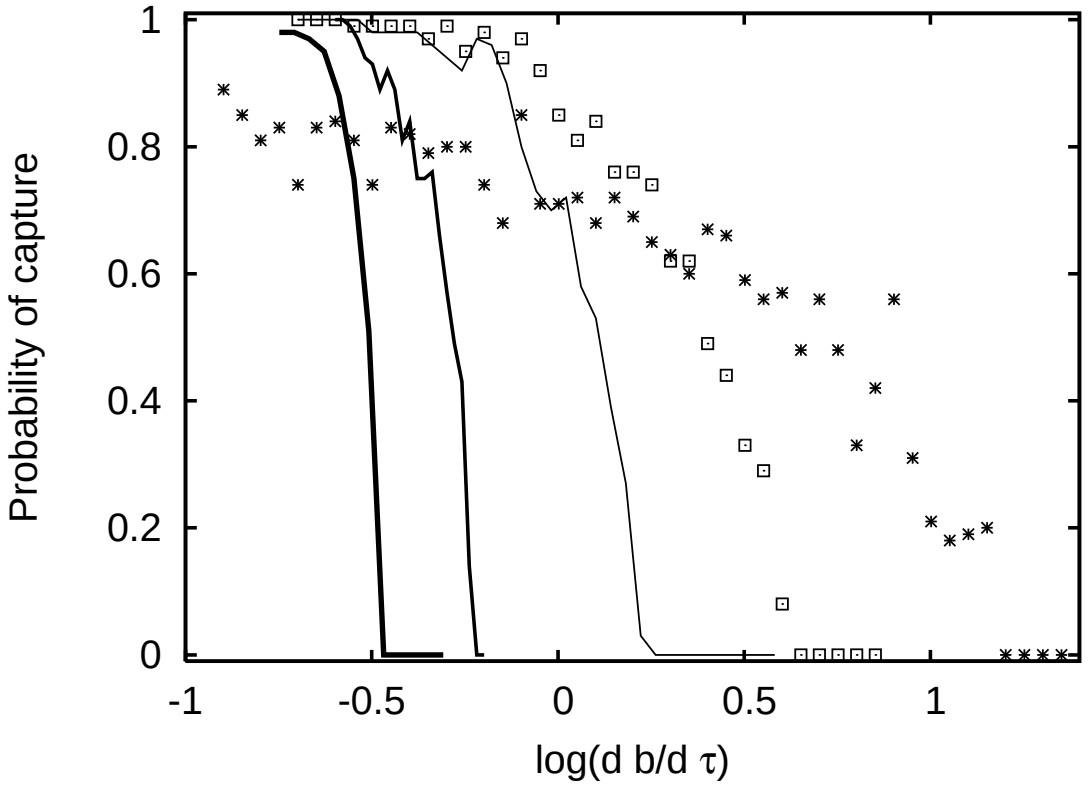

FIG. 3.— Similar to Figure 3 except for the second order resonances (Equation 8 with $k = 2$). The thick, intermediate and thin solid lines show the capture probability for $\bar{\Gamma}(t_0) = 10^{-6}, 10^{-4}$ and 10^{-2} respectively. The squares and stars show the capture probability for $\bar{\Gamma}(t_0) = 0.1$ and 1.0 respectively. Capture is ensured in the adiabatic limit for $\bar{\Gamma}(t_0) < 1/8$. As was true for the first order resonances the transition between capture and no capture is steeper (covering a narrower range in drift rate) for low initial momentum. For second order resonances the drift rate for a capture probability of 0.5 depends on the initial momentum.

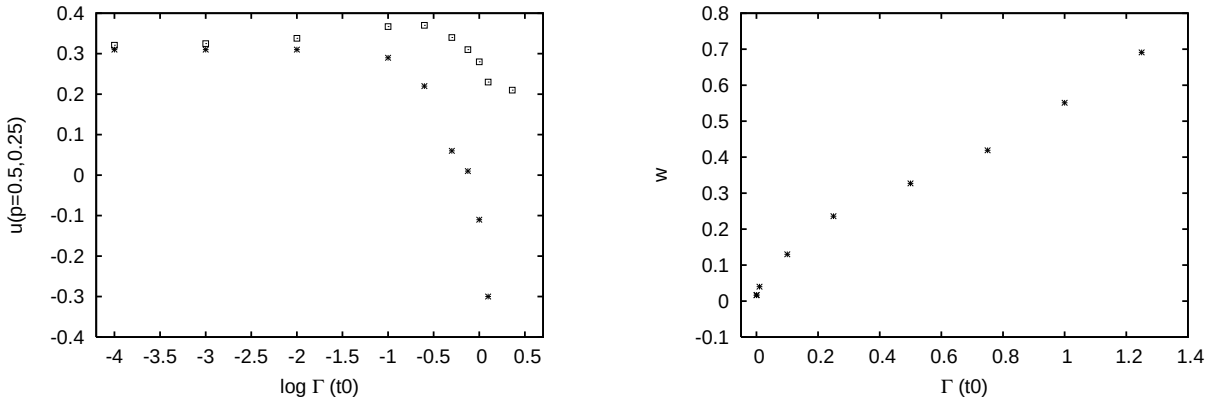

FIG. 4.— a) The drift rate at which the probability of capture is 1/2 (stars) and 1/4 (squares) as a function of initial momentum ($\bar{\Gamma}(t_0)$) for first order resonances ($k = 1$). The x-axis shows $\log_{10} \bar{\Gamma}(t_0)$. The y-axis shows $\log_{10} \left| \frac{d\bar{b}}{d\tau} \right|$. b) Width of the drop in probability as a function of initial momentum.

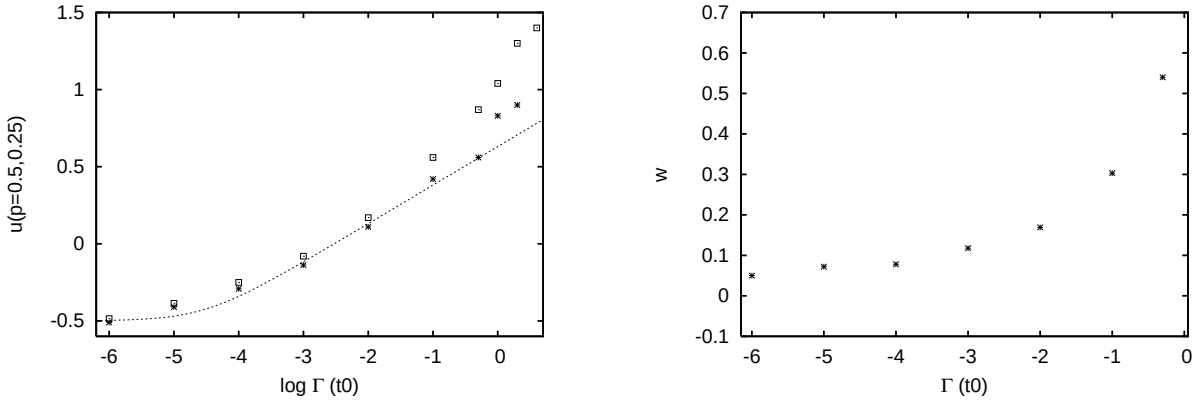

FIG. 5.— a) The drift rate at which the probability of capture is 1/2 (stars) and 1/4 (squares) as a function of initial momentum for first second order resonances ($k = 2$). The x-axis shows $\log_{10} \bar{\Gamma}(t_0)$. The y-axis shows $\log_{10} \left| \frac{d\bar{b}}{d\tau} \right|$. The dotted line shows the function given in Equation (12). b) Width of the drop in probability as a function of initial momentum.

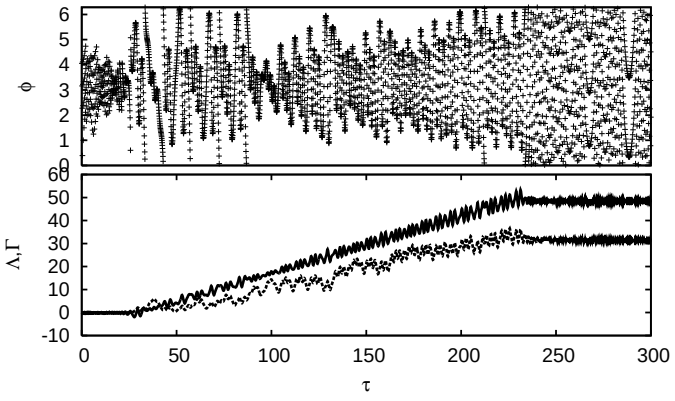

FIG. 6.— The Hamiltonian system with two resonant terms can also exhibit temporary captures. Here Equation (8) is integrated as it passes through resonance. with $\bar{\epsilon} = 1.8$, $\frac{d\bar{b}}{d\tau} = 0.5$, $\bar{c} = 0.9$ and $\bar{\Gamma}(t_0) = 10^{-4}$. The momenta $\bar{\Lambda}$ and $\bar{\Gamma}$ are shown as a solid and dotted lines, respectively.

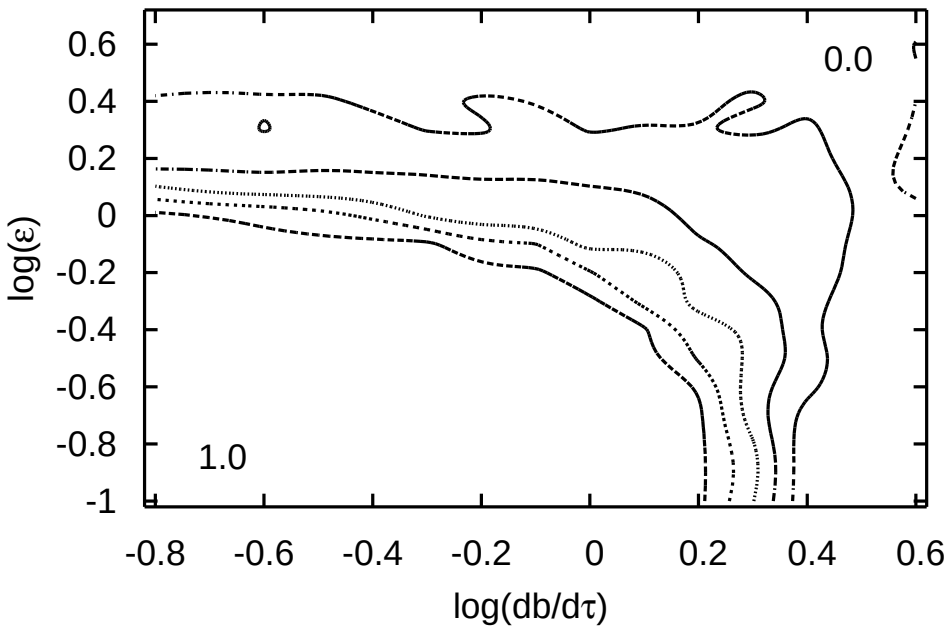

FIG. 7.— The capture probability for a first order resonance ($k = 1$) is shown as a function of drift rate $|\frac{d\bar{b}}{d\tau}|$ and strength of secondary resonance $\bar{\epsilon}$. Contours are shown at probabilities of $0.15, 0.35, 0.55, 0.75$ and 0.95. The numbers 0.0 and 1.0 on the top right and lower left, respectively are placed to make it clear where the probability of capture is near zero and near 1. Equation (16) was numerically integrated with resonance separation $\bar{c} = 0$, and low initial momentum $\bar{\Gamma}(t_0) = 10^{-4}$. Each probability was measured from 100 different trials with randomly chosen initial angles. The x-axis shows $\log_{10}|\frac{d\bar{b}}{d\tau}|$ and the y-axis shows $\log_{10}(\bar{\epsilon})$. For low values of corotation perturbation strength, $\bar{\epsilon}$, the transition between capture and no capture happens at the critical value of $\frac{d\bar{b}}{d\tau}$ estimated for the case of a single perturbation. Near the critical drift rate the additional resonant perturbation can cause a moderately large region with an intermediate probability of capture. At lower drift rates, the corotation resonance prevents capture for $\bar{\epsilon} \gtrsim 1$. To the upper right on this plot (large drift rates and large $\bar{\epsilon}$ values), temporary capture can take place, making it more difficult to measure absolute capture probabilities.

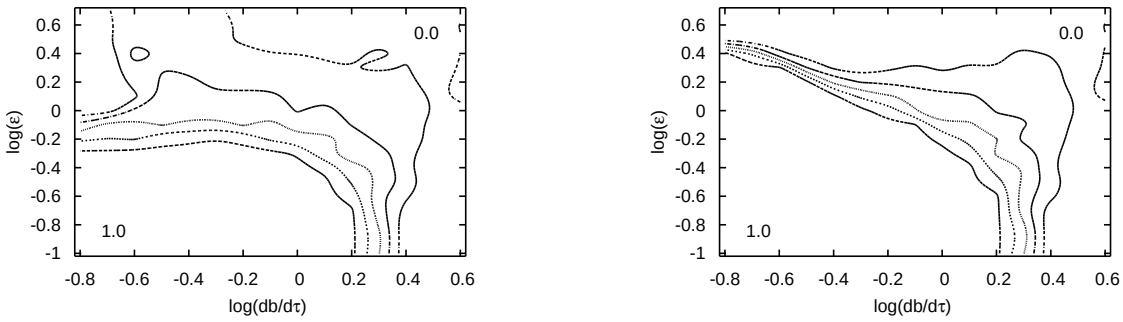

FIG. 8.— a) Same as Fig 7 except the resonance separation $\bar{c} = -0.1$. The frequency of the corotation term is shifted so that this resonance is encountered after the e-resonance. The onset of the corotation resonance can kick the particle out of resonance. b) Same as Fig 7 except the resonance separation $\bar{c} = 0.1$. The frequency of the corotation term is shifted so that this resonance is encountered first. At lower drift rates larger $\bar{\epsilon}$ is required to prevent captures. These figures show that the subresonance separation can influence the capture probability. The subresonance separation is set by the difference between the planet and particle's precession rate of longitude of periapse.

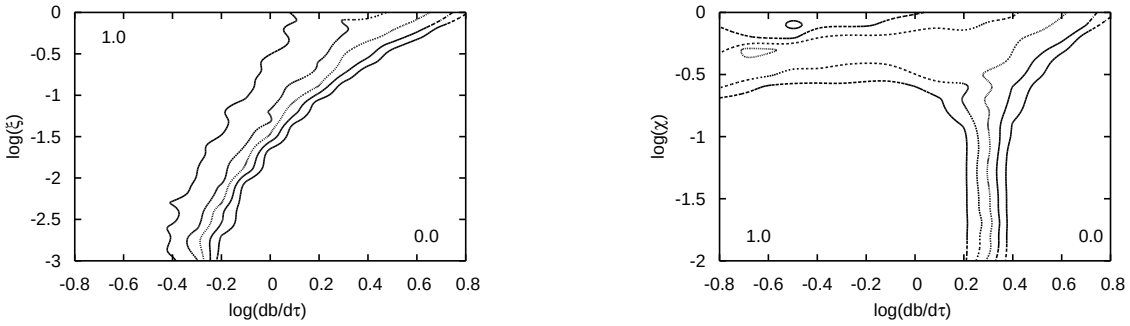

FIG. 9.— a) The capture probability for a second order resonance ($k = 2$) as a function of drift rate and ee'-resonance strength. This figure is similar to Fig. 7. The Equation (18) was numerically integrated with resonance separation $\bar{c}_\xi = 0$, no corotation term, $\bar{\epsilon}_\xi = 0$, and initial momentum $\bar{\Gamma}(t_0) = 10^{-6}$. Drift rate and $\bar{\xi}$ were varied. The x-axis is $\log_{10}|\frac{d\bar{b}_\xi}{d\tau}|$ and the y-axis is $\log_{10}(\bar{\xi})$. For low ee'-resonance strength or $\bar{\xi} \lesssim 10^{-3}$, the capture probability drops at a drift rate consistent with the critical value measured in section 3 for a single second order resonance (Equation 11). For larger values of ee' resonant term, $\bar{\xi}$, the critical drift rate increases, depending upon $\bar{\xi}$. In this case the system fails to capture into the second order e^2-resonance and instead captures into ee'-resonance which behaves like a first order resonance. b) The Equation (19) was numerically integrated with $\bar{c}_\chi = 0$, $\bar{\epsilon}_\chi = 0$, and initial momentum $\bar{\Gamma}(t_0) = 10^{-6}$. Drift rate and $\bar{\chi}$ were varied. The x-axis is $\log_{10}|\frac{d\bar{b}_\chi}{d\tau}|$ and the y-axis is $\log_{10}(\bar{\chi})$. Because $\chi = \xi^{-2/3}$ this figure covers large values of ξ, extending past the top of a). For low e^2-resonance strength or $\bar{\xi} \lesssim 10^{-1}$, the capture probability drops at a drift rate consistent with that predicted in section 3 for a single first order resonance; (Equation 11). For $\bar{\chi} \sim 0.5$ there is a regime of drift rates with intermediate capture probability.

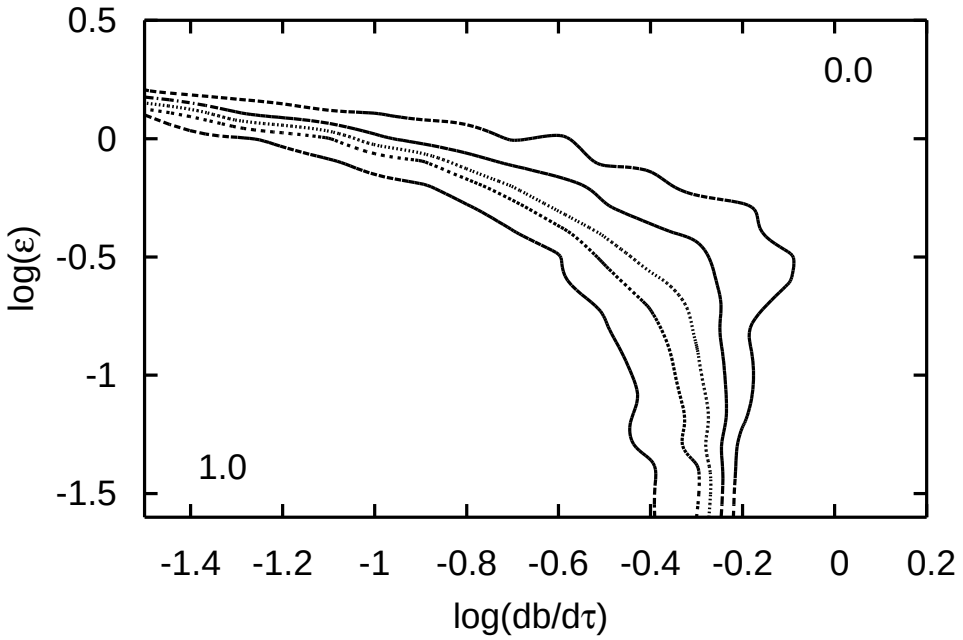

FIG. 10.— The capture probability for a second order resonance ($k = 2$) as a function of drift rate and corotation resonance strength. This figure is similar to Fig. 7. The Equation (18) was numerically integrated with $\bar{c}_\xi = 0$, $\bar{\xi} = 0$, and initial momentum $\bar{\Gamma}(t_0) = 10^{-6}$. Drift rate and $\bar{\epsilon}_\xi$ were varied. The x-axis is $\log_{10}|\frac{d\bar{b}_\xi}{d\tau}|$ and the y-axis is $\log_{10}(\bar{\epsilon}_\xi)$. At low values of $\bar{\epsilon}_\xi$ the capture probability drops at a value consistent with that predicted in section 3 for a single second order resonance; Equation (11). At $\bar{\epsilon}_\xi \sim 1$ the corotation terms prevents capture into the e^2-resonance.

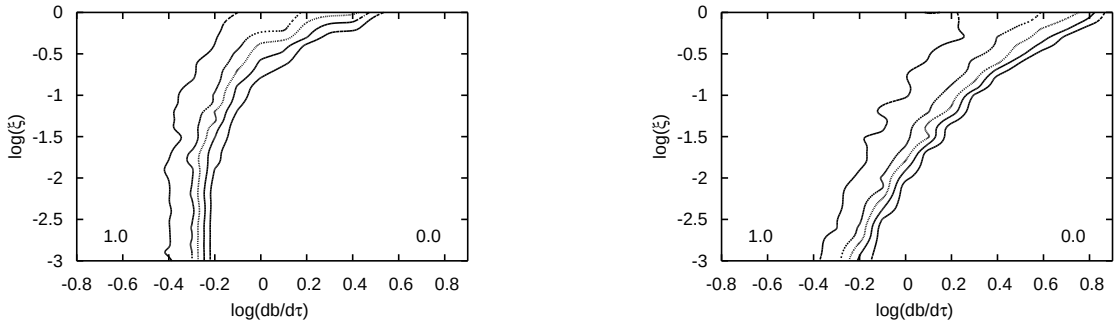

FIG. 11.— Separated second order resonances. a) This Figure is similar to Figure 9a except $\bar{c}_\xi = -1$. The ee'-resonance is encountered after the e^2-resonance. b) This Figure is similar to Figure 9a except $\bar{c}_\xi = 1$. The ee'-resonance is encountered before the e^2-resonance.

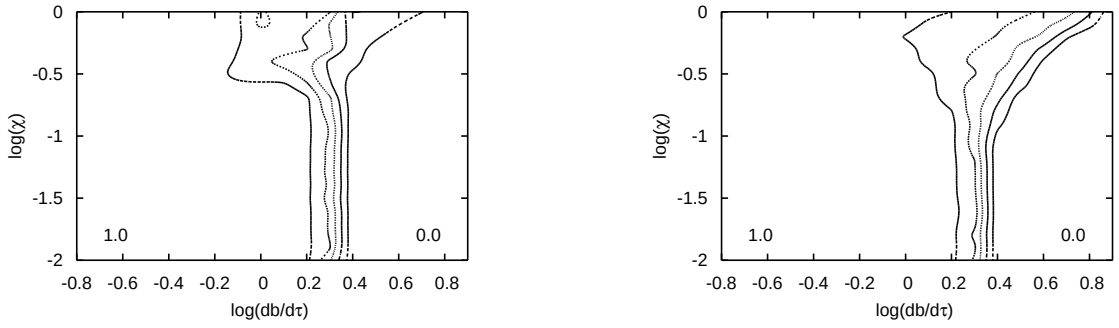

FIG. 12.— Separated second order resonances. a) This Figure is similar to Figure 9b except $\bar{c}_\chi = -0.5$. The ee'-resonance is encountered before the e^2-resonance. b) This Figure is similar to Figure 9b except $\bar{c}_\chi = 0.5$. The ee'-resonance is encountered after the e^2-resonance.

TABLE 1
COEFFICIENTS FOR $k = 1$ RESONANCES

	Exterior resonances			Interior resonances		
$j : k$	4:3	3:2	2:1	4:3	3:2	2:1
α	0.825	0.763	0.630	0.825	0.763	0.630
a	−16.35	−7.86	−2.38	−19.81	−10.30	−3.78
c/μ	−4.14	−2.01	−0.61	−5.02	−2.64	−0.98
$\delta_{1,0}/\mu$	−3.41	−2.31	−0.24	−4.21	−3.06	−1.89
$\delta_{1,1}/(\mu e_p)$	2.35	1.55	0.75	3.07	2.29	0.31
$\dot{n}_{p,crit}/\mu^{4/3}$	198.5	48.4	0.54	398.7	126.4	22.7
$\bar{\epsilon}/(\mu^{-1/3}e_p)$	1.16	1.00	6.59	1.22	1.21	0.21
$\bar{c}/\mu^{1/3}$	0.72	0.58	1.18	0.71	0.58	0.41
$e_{lim}/\mu^{1/3}$	0.98	1.08	0.72	1.08	1.24	1.54

NOTE. — Equations (2) and (4) were used to calculate the coefficients a and c (for external resonances). Equations (A2) and (A3) were used to estimate the perturbation strengths for the 4:3 and 3:2 resonances and the 2:1 resonance, respectively, for external resonances. Coefficients for the internal resonances are given in the appendix. The critical drift rate is calculated from Equation (14). The coefficients $\bar{\epsilon}$ and $\bar{c}$ are calculated from Equation (17). We have calculated c using only the secular term from one planet and assumed that $\dot{\varpi}_p = 0$. The critical eccentricity ensuring capture in the adiabatic limit is calculated using Equation (A4).

TABLE 2
COEFFICIENTS FOR $k = 2$ RESONANCES

	Exterior resonances		Interior resonances	
$j : k$	3:1	5:3	3:1	5:3
α	0.481	0.711	0.481	0.711
a	−3.12	−18.98	−6.49	−26.68
c/μ	−0.20	−1.22	−0.41	−1.72
$\delta_{2,0}/\mu$	0.24	6.82	0.63	3.47
$\delta_{2,1}/(\mu e_p)$	−1.25	−8.00	−3.76	−13.33
$\delta_{2,2}/(\mu e_p^2)$	0.10	1.04	0.36	5.69
$\bar{\xi}/(\mu^{-1/2}e_p)$	18.56	1.95	19.11	10.61
$\bar{\epsilon}_\xi/(\mu^{-1}e_p^2)$	5.59	0.43	5.93	12.56
$\bar{c}_\xi/\mu^0$	0.81	0.18	0.65	0.50
$\dot{n}_{p,crit,\xi}/\mu^2$	0.029	69.86	0.60	30.19
$e_{lim,\xi}/\mu^{1/2}$	0.40	0.95	0.19	0.20
$\bar{\epsilon}_\chi/(\mu^{-1/3}e_p^{2/3})$	0.114	0.174	0.116	0.538
$\bar{c}_\chi/(\mu^{1/3}e_p^{-2/3})$	0.12	0.11	0.09	0.10
$\dot{n}_{p,crit,\chi}/(\mu^{4/3}e_p^{4/3})$	5.77	683	40.66	1694
$e_{lim,\chi}/(\mu^{1/3}e_p^{1/3})$	1.06	1.19	1.73	1.50

NOTE. — Equations (2) and (4) were used to calculate a and c. The critical drift rates $\dot{n}_{p,crit,\xi}$ and $\dot{n}_{p,crit,\chi}$ are those calculated for low $\bar{\xi}$ and $\bar{\chi}$ respectively. $\dot{n}_{p,crit,\xi}$ is given in the limit of low initial particle eccentricity. For particle initial eccentricity near the limit ensuring capture in the adiabatic limit, the values given here for $n_{p,crit,\xi}$ should be multiplied by 10. The coefficients $\bar{\epsilon}_\xi$, and $\bar{c}_\xi$ are calculated from Equation (19). The coefficients $\bar{\epsilon}_\chi$, and $\bar{c}_\chi$ are calculated from Equation (20). Expressions from the appendix were used to calculate the δ coefficients and critical eccentricities. We have calculated c using only the secular term from one planet and assumed that $\dot{\varpi}_p = 0$.